

High Precision Hybrid Pulse and Phase-Shift Laser Ranging System

Peijia Yan

A Thesis

in

The Department

of

Electrical and Computer Engineering

Presented in Partial Fulfillment of the Requirements

For the Degree of Master of Applied Science at

Concordia University

Montreal, Quebec, Canada

October, 2018

© Peijia Yan, 2018

**CONCORDIA UNIVERSITY
SCHOOL OF GRADUATE STUDIES**

This is to certify that the thesis prepared

By: **Peijia Yan**

Entitled: "High Precision Hybrid Pulsed and Phase-Shift Laser Ranging System"

and submitted in partial fulfillment of the requirements for the degree of

Master of Applied Science

Complies with the regulations of this University and meets the accepted standards with respect to originality and quality.

Signed by the final examining committee:

_____ Chair
Dr. Y. Zhang

_____ Examiner, External
Dr. Y. Zhang (MIE) To the Program

_____ Examiner
Dr. S. Shih

_____ Supervisor
Dr. J. X. Zhang

Approved by: _____
Dr. W. E. Lynch, Chair
Department of Electrical and Computer Engineering

_____ 20

_____ Dr. Amir Asif, Dean
Faculty of Engineering and Computer
Science

ABSTRACT

High Precision Hybrid Pulsed and Phase-Shift Laser Ranging System

Peijia Yan

With the rapid development of military, aerospace, and precision manufacturing technology, a multitude of situations need to carry out a large-range and high-precision distance measurement. The growth of measurement applications has led to a higher requirement for the laser ranging technology which can be accomplished by using different patterns. At present, the pulse laser ranging method is widely used for medium-range and long-range measurement because of the fast measurement speed and considerable measurement range. However, the ranging precision is low. The short-distance measurement mostly adopts the phase-shift laser ranging method which has high ranging accuracy but limited measurement range. Therefore, the research on lifting the accuracy of pulse laser ranging method and extending the measurement range of the phase-shift laser ranging method will be carried out.

In this thesis, combining the existing pulse laser ranging system and phase-shift laser ranging system, dual-frequency and single-frequency hybrid pulse and phase-shift laser ranging systems are proposed. The basis for solving the current problems of poor measurement precision in pulse laser ranging method and short measurement distance in phase-shift laser ranging method are provided. Also, the designed structures have a broad application prospect in the fields of industrial production, military, and aviation.

At the beginning of the thesis, the principle and characteristics of the current typical laser ranging methods are introduced and analyzed. According to the Fourier Series theory, the spectrum analysis of the pulse signal and the relationship between the pulse signal and the same-frequency sinusoidal signal, the idea of phase-shift laser ranging based on pulse modulation signal is generated. Instead of a continuous sinusoidal signal, the laser is modulated with a periodic pulse signal. Distance measurement by calculating the phase difference on the sinusoidal signal extracted from the pulse signal with the same frequency at the receiving end.

Based on the principle of conventional dual-frequency phase-shift laser ranging method, a dual-frequency pulse laser ranging method is proposed. The distance to be measured is obtained by transmitting two periodic pulse signals with different frequency and then combining the implementation of rough and accurate measurement outcomes. Afterward, a single-frequency pulse laser ranging method is introduced. After receiving the pulse signal, the direct counter method is used to realize rough measurement and phase-shift of the co-frequency sinusoidal signal is utilized to improve the ranging accuracy. This proposed model has the advantages of high ranging precision and long-distance measurement without any other auxiliary frequency.

The accuracy of the phase difference calculation is the most critical element in both the dual-frequency and single-frequency laser ranging systems. Currently, the commonly used phase difference calculation methods operated in phase-shift laser ranging system are digital synchronous detection, fast Fourier transform method, and all phase fast Fourier transform method. Published works have discussed the performance of frequency estimation and initial phase calculation using these approaches. In this thesis, the precision of phase difference measurement based on these methods above is compared. The effects of normalized frequency deviation, white Gaussian noise, harmonics are simulated in MATLAB. Simulation results show that all phase fast Fourier transform method has a superior anti-noise ability so that exceptional accuracy of phase difference measurement can be achieved. Furthermore, as the number of sampling points increases, all phase fast Fourier transform method will obtain a more accurate calculation consequence.

Finally, this thesis carries on the co-simulation test of the designed dual-frequency and single-frequency hybrid pulse and phase-shift laser ranging systems in Optisystem and MATLAB. The transmitting frequencies of pulse signals operated in the dual-frequency method are 15 MHz and 150 KHz. The pulse used in the single-frequency method is set to 15 MHz. In the simulation, the performance of proposed methods is tested by setting various measuring distance. When the number of sampling points is 1024, the standard deviation and ranging error of the dual-frequency method are 3.72 cm and 13.6 cm within 963.15 meters. For the single-frequency method, the results show a 3.78 cm standard deviation and 14.6 cm ranging error. Simulation results illustrate that the proposed ranging methods have lower ranging error compared with recently published works. It means that the combination of the pulse method and the phase-shift method can achieve high-accuracy and long-range measurement.

ACKNOWLEDGEMENTS

I would like to show my sincerest thankfulness and appreciation to Professor John Xiupu Zhang for making valuable guidance for my thesis. Thank him for providing me with a valuable research project and carefully supporting me to finish the research.

I would like to express my appreciations to my colleague Lara A.Juras and Khan, for their endless assistance and support in the Optisystem and MATLAB simulation.

I would like to thank my colleagues Hao Sun and Xiaoran Xie in the laboratory. In the lab, I learned a lot of knowledge and skills, very grateful to them for their care and help in the past two years.

I would like to say huge thanks to my parents, Jianwei Yan and Weiping Xu, for their selfless dedication and endless love during my study in Canada.

Table of Contents

List of Figures	ix
List of Tables	xi
List of Acronyms	xii
Chapter 1 Introduction	1
1.1 Development and Present Situation of Laser Ranging System	1
1.1.1 The Development of Laser Ranging Technology	1
1.1.2 Characteristics and Classification of Laser Ranging System	2
1.1.3 Development Trend of Laser Ranging System	3
1.2 Thesis Outline	4
Chapter 2 Background and Literature Review	6
2.1 Laser Ranging Technologies	6
2.1.1 Laser	6
2.1.2 Optical Modulators	7
2.1.3 Optical Receiver	8
2.1.4 Multi-Beam LIDAR	8
2.2 Triangulation Method	9
2.3 Interference Method	11
2.4 Frequency Modulation Continuous Wave	13
2.5 Time-of-Flight Method	16
2.5.1 Time Discrimination Method	17
2.5.2 Time Interval Measurement Method	19
2.5.3 Applications of Time-of-Flight Method	21
2.6 Phase-Shift Method	22

2.6.1	Phase-Shift Measurement Method	22
2.6.2	Multi-Value Problem of Phase-Shift Ranging System.....	23
2.6.3	Applications of Phase-Shift Method	26
2.7	Comparison of Laser Ranging Method	27
2.8	Motivation and Contribution.....	28
Chapter 3	Analysis and Design of Hybrid Pulse and Phase-Shift Laser Ranging System	30
3.1	Combination of Pulse Method and Phase-Shift Method.....	30
3.1.1	Fourier Series of Pulse Signal	30
3.1.2	Heterodyne Detection Technology.....	35
3.1.3	Beam Divergence	37
3.1.4	Reflectivity.....	38
3.1.5	Transmission Module	39
3.2	Phase Measurement Method	40
3.2.1	Digital Synchronous Detection	40
3.2.2	Fast Fourier Transform Method	42
3.2.3	Ap-FFT Phase Measurement Method	44
3.3	Design of Dual-Frequency Pulse Laser Ranging System	47
3.3.1	Frequency Selection Principle.....	50
3.4	Design of Signal-Frequency Pulse Laser Ranging System.....	51
3.4.1	Frequency Selection Principle.....	53
3.5	Error Analysis of Measurement System.....	54
3.5.1	Light Velocity Error	54
3.5.2	Influence of Modulation Frequency	54
3.5.3	Phase Measurement Error	55
Chapter 4	Simulation of Phase-Detection Performance and Laser Ranging System	58
4.1	Simulation of Phase-Detection Performance	58
4.1.1	The effect of Frequency Offset	58

4.1.2	The Effect of White Gaussian Noise	61
4.1.3	The Effect of Harmonic.....	62
4.1.4	The Effect of Frequency Offset, White Gaussian Noise and Harmonics	63
4.1.5	The Influence of Sampling Points on Phase Accuracy.....	65
4.2	Simulation of Laser Ranging System.....	66
4.2.1	Dual-Frequency Hybrid Pulse and Phase-Shift Laser Ranging Model	67
4.2.2	Single-Frequency Hybrid Pulse and Phase-Shift Laser Ranging Model	71
4.3	Laser Ranging System Comparison	74
4.4	Simulation Summary.....	77
Chapter 5	Conclusion	78
5.1	Thesis Conclusion	78
5.2	Future Work	79
Reference	81

List of Figures

Figure 2-1 Typical structure of a semiconductor laser [8].....	6
Figure 2-2 The structure of direct modulation.....	7
Figure 2-3 The structure of a transmitter using an external modulator	7
Figure 2-4 The structure of an optical receiver.....	8
Figure 2-5 A picture of raw data from HDL-64E.....	9
Figure 2-6 Conceptual image of the passive triangulation	10
Figure 2-7 Conceptual image of the active triangulation.....	11
Figure 2-8 Conceptual image of the interference method	12
Figure 2-9 Conceptual image of the FMCW method	14
Figure 2-10 Relation between beat frequency and time in the FMCW method	15
Figure 2-11 Conceptual image of TOF.....	16
Figure 2-12 Leading edge discriminator.....	18
Figure 2-13 Constant fraction discriminator.....	18
Figure 2-14 Conceptual image of the phase-shift method.....	22
Figure 2-15 Principle of the modulated laser propagating on the measured distance	24
Figure 2-16 Diagram of ETS-VII distance measurement system [68].....	26
Figure 3-1 Pulse signal $f(t)$ and Fourier Series coefficients C_n when $\tau_1 = \frac{1}{20}s, T_1 = \frac{1}{4}s$	33
Figure 3-2 Pulse signal $f(t)$ and Fourier Series coefficients C_n when $\tau_2 = \frac{1}{20}s, T_2 = \frac{1}{2}s$	34
Figure 3-3 Pulse signal $f(t)$ and Fourier Series coefficients C_n when $\tau_3 = \frac{1}{8}s, T_3 = \frac{1}{2}s$	35
Figure 3-4 The principle of heterodyne detection technology.....	36
Figure 3-5 The geometric representation of the transmitting beam and reflected beam [73].....	37
Figure 3-6 The reflection model of diffuse objects [73].....	38
Figure 3-7 The principle of digital synchronous detection.....	41
Figure 3-8 The principle of the ap-FFT method	45
Figure 3-9 The principle of data preprocessing	47
Figure 3-10 Model of dual-frequency pulse laser ranging system	47
Figure 3-11 Model of signal-frequency pulse laser ranging system.....	52

Figure 3-12 The effect of phase measurement error on distance measurement error.....	56
Figure 4-1 Error of measurement with different phase shift at 9.99 KHz	59
Figure 4-2 Error of measurement with different phase shift at 10.01 KHz	59
Figure 4-3 Comparison of phase error under frequency offset.....	60
Figure 4-4 Mean value of phase shift measurement under white Gaussian noise	61
Figure 4-5 Comparison of phase error under white Gaussian noise.....	62
Figure 4-6 Comparison of phase error with harmonics	63
Figure 4-7 Mean value of phase shift measurement	64
Figure 4-8 Comparison of phase error under frequency offset, white Gaussian noise and harmonics	64
Figure 4-9 Comparison of phase error with different sampling points.....	65
Figure 4-10 Simulated dual-frequency hybrid pulse and phase-shift laser ranging system	67
Figure 4-11 Waveforms of the reference and measurement signal when the signal frequency is 150 KHz.....	68
Figure 4-12 Waveforms of the reference and measurement signal when the signal frequency is 15 MHz.....	68
Figure 4-13 Phase difference between the reference signal and measured signal when the signal frequency is 150 KHz	69
Figure 4-14 Phase difference between the reference signal and measured signal when the signal frequency is 15 MHz	69
Figure 4-15 Distance measurement result when the ranging distance is 100m.....	70
Figure 4-16 Simulated single-frequency hybrid pulse and phase-shift laser ranging system.....	71
Figure 4-17 Pulse counting part in Simulink	72
Figure 4-18 Phase difference between the reference signal and measured signal when the signal frequency is 15 MHz	72
Figure 4-19 Phase difference between the reference signal and measured signal.....	73
Figure 4-20 Distance measurement result when the ranging distance is 100m.....	73

List of Tables

Table 1-1 Typical laser rangefinder.....	3
Table 2-1 Comparison of commonly used ranging methods.....	28
Table 3-1 The reflectance of a laser with a wavelength of 900 nm to distinct objects [75].....	38
Table 3-2 Mixing result of the received signal and reference signals	42
Table 3-3 Maximum unambiguous range and ranging resolution of two frequencies	51
Table 3-4 Crystal oscillator product data.....	55
Table 4-1 Main simulation parameters	66
Table 4-2 Simulation results of the dual-frequency hybrid pulse and phase-shift laser ranging model	70
Table 4-3 Simulation results of the single-frequency hybrid pulse and phase-shift laser ranging model	74
Table 4-4 The simulation results of the standard deviation of ranging error.....	75
Table 4-5 The simulation results of worst ranging error	75
Table 4-6 Ranging errors reported from [35]	76
Table 4-7 Ranging errors reported from [93]	76

List of Acronyms

A/D	Analog to Digital
AP-FFT	All Phase Fast Fourier Transform
APD	Avalanche Photo Diode
CCD	Charge-Coupled Device
CMOS	Complementary Metal Oxide Semiconductor
DFT	Discrete Fourier Transform
ERS-2	European Remote-Sensing Satellite
ESA	European Space Agency
FFT	Fast Fourier Transform
FMCW	Frequency Modulation Continuous Wave
GEOSAT	Geodetic Satellite
LIDAR	Light Detection and Ranging
NAR	Non-Ambiguity Range
PBS	Polarity Beam Splitter
PD	Photo Detector
PIN	P-I-N Photodiode
PMT	Photomultiplier Tube
SLAM	Simultaneous Localization and Mapping
Si-APD	Silicon Avalanche Photodetectors
TOF	Time of Flight
VCO	Voltage-Controlled Oscillator

Chapter 1 Introduction

1.1 Development and Present Situation of Laser Ranging System

1.1.1 The Development of Laser Ranging Technology

The term “Laser” is an acronym for "light amplification by stimulated emission of radiation" which is a remarkable invention of humanity in the twentieth century [1]. In 1916, Einstein proposed the famous theory of stimulated emission, which is the reason why the laser can produce light [2]. The principle of stimulated emission is that if the particles in the high energy state are exposed to the external photons, the particle will transit from the high energy state to the low energy state, then the particles will radiate the photons.

Laser ranging technology is the earliest application of laser in the military [3]. The research of laser rangefinder began in the 20th century, 60 years. In 1961, Robert W. Hellwarth of Hughes Research Labs produced the world's first laser rangefinder. In 1962, the world's first military laser range finder successfully demonstrated the performance; laser rangefinder can indeed be used as a new type of distance measurement method instead of the original optical range finder. In 1969, laser rangefinder was first equipped in the US forces. Since then, various models of military laser rangefinders have been powered by national troops.

After 20-year development, the mid-80s has solved the variety of the leading technical issues of optical devices, optical systems, and signal processing circuits. To the late 90s, military laser rangefinder has been equipped for the second generations, developed to the third generation. Third-generation laser rangefinder which is human-eye-safety laser rangefinder has been developed into the working wavelength of 1.06 μm and 1.54 μm . Several types of human-eye-safety laser rangefinders have entered the production and application stage [4].

Concurrently, laser ranging technology has gradually applied to civilian areas. From the early 1970s to the present, nearly 50 years, many universities, research institutes and companies have also carried out this research work. Research directions include laser ranging subsystems and

their applications and products related to industry, engineering, aerospace, robot vision, navigation and many other aspects.

1.1.2 Characteristics and Classification of Laser Ranging System

Compared with the ultrasonic rangefinder, laser range finder has the features of fast measurement speed, high measurement precision, and easy aiming. If the use of a continuous laser as a light source, it can get an exceptional measurement accuracy which is mainly used for short-range measurement [5]. If a pulsed laser is operated as a light source, the accuracy of the laser rangefinder is small. However, when the pulsed laser utilized for long-distance measurement, it can achieve a high relative measurement precision.

According to the characteristics of the instrument, the laser rangefinder can be divided into the following categories:

Laser tracker: the accuracy of the distance measurement is related to the performance of the laser interferometer. In theory, the accuracy can reach 0.01 mm when the measured distance is less than 10 m. It is a combination of laser ranging interferometer and the total station with automatic angle measurement, which can be used to measure stationary targets, track and measure moving targets.

Laser total station: the ranging distance of short-distance ranging total station is less than 2 km and mainly used for ordinary measurement and urban analysis. It is a surveying and mapping instrument system which integrates analysis functions of horizontal angle, vertical angle, distance (slant distance, horizontal distance) and height difference.

Telescope laser rangefinder: the measuring distance of the telescope laser rangefinder is 600~3000m. The measurement distance is relatively far, but the ranging accuracy typically can only achieve 1m. So, the telescope laser rangefinder is mainly used for outdoor long-distance measurement.

Handheld laser rangefinder: the measuring range is generally less than 200 meters, and the measurement veracity is about 3 mm. Currently, the handheld laser rangefinder is the most widely

used laser rangefinder [6]. Other than measuring the distance, it can also calculate the volume of the measured object.

Some representative laser rangefinders are shown in Table 1-1.

Table 1-1 Typical laser rangefinder

Model	Manufacturer	Measuring range(m)	Measurement accuracy(mm)
D5	Leica	0.05~200	±1.0
DLE40	BOSCH	0.05~40	±1.5
GLM250	BOSCH	0.05~250	±1.0
411D	Fluke	0.1~30	±3.0
SP2000H	Trueyard	10~2000	±1000
1800A	ORPHA	15~1800	±1000±0.1%
202540	Bushnell	5~1760	±500
LRM2200SI	NEWCON	20~2200	±1000

1.1.3 Development Trend of Laser Ranging System

With the development of aircraft, shipbuilding, bridges and other industries and the extensive application of measuring instruments, the improvement of laser distance measuring devices tends to be high precision and long distance. The laser distance measurement devices are not limited to distance measurement, but it can also combine with the robust application software to analyze the measurement data such as angle, and height.

1. High precision and long distance

The ranging requirements of different projects are not identical. In general, the range is in the hundreds of meters, and the accuracy requirement is between centimeters and millimeters. For some industrial measurement fields, a high-precision and long-distance measurement equipment is required to reach the ranging distance of 1000 meters and the measurement accuracy of centimeters.

2. High sampling rate

With the advancement of measurement technologies, the control system requires fast data transmission capacity of thousands of points per second to achieve accurate data processing and improve the efficiency of analysis.

1.2 Thesis Outline

The rest chapters are as follows:

In chapter 2, the commonly used schemes of laser ranging technology, including triangulation method, interference method, frequency modulation continuous wave method, time-of-flight (pulse) method, and the phase-shift method are discussed. After that, the differences between these methods are analyzed and compared. The problems existing in the current laser ranging systems are investigated.

In chapter 3, the principle of the pulse method and the phase-shift method are discussed. The relationship between the pulse signal and the sinusoidal signal with the same frequency are presented. Accordingly, the pulse signal is selected as the modulation signal in the phase-shift laser ranging system. The commonly used phase discrimination methods are introduced: digital synchronous detection, fast Fourier transform method and all phase fast Fourier transform method. Based on the principle of dual-frequency phase-shift laser ranging system, dual-frequency pulse laser ranging system and single-frequency pulse laser ranging system are proposed. Then, according to the relationship between the measurement distance and the ranging accuracy, the modulation frequency is determined.

Chapter 4 compares the phase measurement accuracy of above three measurement methods in different conditions by MATLAB simulation. Through comparison and analysis, the all phase fast Fourier transform method can get higher phase difference accuracy under different circumstances. Then, to verify the feasibility and correctness of two proposed laser ranging systems designed in this thesis, simulation experiments are executed in Optisystem-MATLAB co-simulation. The simulation results reveal that the proposed systems can achieve high precision laser ranging.

In chapter 5, the research and innovation in this thesis are summarized. The shortcomings of the current research and the improvement direction are introduced.

Chapter 2 Background and Literature Review

This chapter presents the typical laser ranging schemes. In general, a laser ranging system consists of three parts which are the laser emission unit, the receiving unit, and the distance calculation unit. The emission unit is composed of two parts: one is the frequency synthesizing part, and the other one is the laser emitting part. The receiving unit includes a photoelectric receiving part and several signal processing circuits. Due to the difference of system components, the various laser ranging schemes and their applications are discussed in this chapter.

2.1 Laser Ranging Technologies

2.1.1 Laser

The laser is a critical device in the laser ranging device. Currently, lasers are divided into three categories: solid-state lasers, gas lasers, and semiconductor lasers [7]. Solid-state lasers typically have a continuous power of more than 100W and a peak pulse power of up to 10^9 W which is generally used for satellite rangefinder. However, due to the complexity of the working medium, the price is high. Gas lasers have a simple structure, which can produce a variable frequency of laser with stable frequency and amplitude. However, the gas laser is giant, which is generally used for laser collimation, gyroscope, and other measuring instruments. Semiconductor lasers have high output power and high efficiency. It can achieve direct modulation to reach a high modulation frequency. Its structure is simple and it widely used in laser rangefinder and infrared rangefinder equipment. Figure 2-1 shows a typical structure of a semiconductor laser [8].

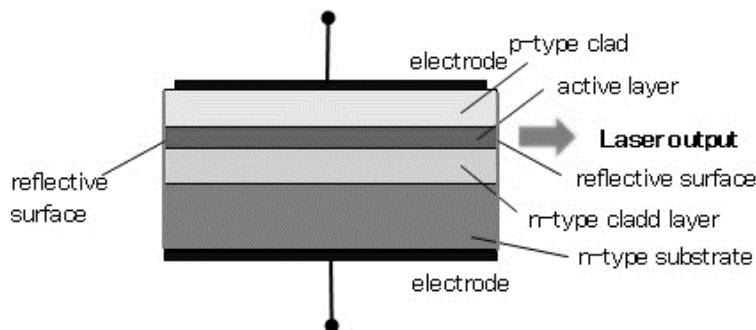


Figure 2-1 Typical structure of a semiconductor laser [8]

2.1.2 Optical Modulators

Optical modulation refers to the optical signal is modulated by a digital signal or an analog signal. Direct modulation and external modulation are two main types of optical modulation approaches [9].

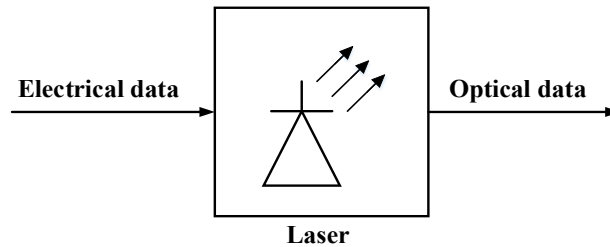


Figure 2-2 The structure of direct modulation

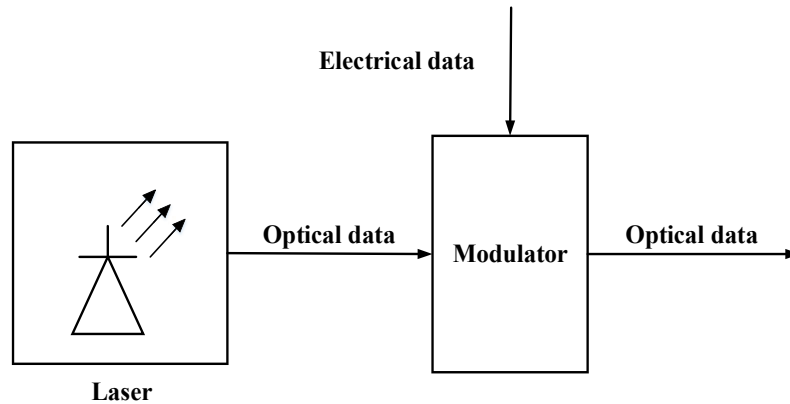


Figure 2-3 The structure of a transmitter using an external modulator

The structure of direct modulation is shown in Figure 2-2, and the typical structure of the transmitter using an external modulator is shown in Figure 2-3. For direct modulation, the current of the laser is modulated by the injection modulation signal. External modulation method separates the laser and the modulator. The modulation signal is injected into the modulator. When the beam emitted by the laser passes through the modulator, the modulated laser beam can be obtained.

The direct modulation method is relatively straightforward and has an uncomplicated structure which can work in the broad frequency range with stable frequency response. Most of the semiconductor lasers applied in rangefinder are directly modulated.

2.1.3 Optical Receiver

The structure of an optical receiver is shown in Figure 2-4. Normally, an optical receiver includes a photodetector (PD), a preamplifier and various signal processing circuits [10].

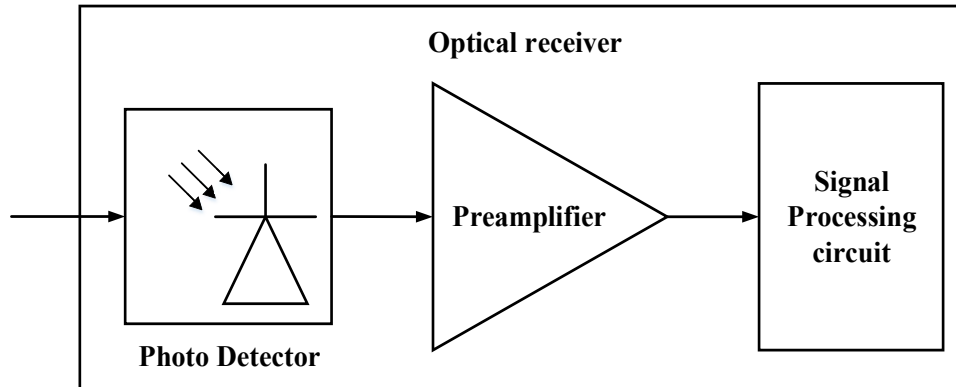


Figure 2-4 The structure of an optical receiver

The received light beam is converted into an electrical current by the photodetector and then passed through the preamplifier. The signal processing circuit can be filters or some passive components. In the laser ranging system, the signal processing circuit is responsible for calculating the measurement distance.

For the photodetector, selectable photoelectric sensors are Photomultiplier Tube (PMT), P-I-N Photodiode (PIN) and Avalanche Photodiode (APD). APD has the characteristics of high gain, exceptional sensitivity, small size, and fast response speed. Moreover, it has gradually replaced the other photodiodes as the most commonly used receiver in laser rangefinder.

2.1.4 Multi-Beam LIDAR

Light Detection and Ranging (LiDAR) is a measurement instrument that using lasers to identify geometric characteristics of objects such as speed, appearance, and position [11]. By processing the received beams, the feature of the measured target such as the range, reflectivity and other elements are demonstrated. Subsequently, the corresponding algorithm can be used to detect the location, height, speed, and posture of the object [12][13]. Typically, LiDAR can achieve a detection accuracy of a few centimeters.

Multi-beam LIDAR has been playing a crucial role in robotic operations such as autonomous vehicles with the popularity of autonomous driving because it is capable of presenting 3D information of the surroundings in real time [14]. Furthermore, multi-beam LIDAR can be effectively operated for projects like localization [15], target detection [16], scene understanding [17], and simultaneous localization and mapping (SLAM) [18].

LiDAR installed on the automobile for positioning and mapping already has a variety of brands. Currently, Velodyne LiDAR has the most mature technology in LiDAR field which has developed a variety of LiDAR products for automotive and topography [19]. The Velodyne HDL-64E is densely installed in robotics which 64-laser channels are mounted on a scanning head rotating with the frequency of 5~20 Hz to acquire 1.3 million 3D data per second. A picture of raw data from HDL-64E is shown in Figure 2-5 [20], where the points illustrate the visual brightness. VLP-16 is widely used in the surveying industry due to its lightweight, little power consumption and excellent efficiency. Nonetheless, Velodyne's LiDAR products are very costly and require more than half a year from production to delivery. Currently, how to reduce costs is the primary consideration of multi-beam LIDAR technology.

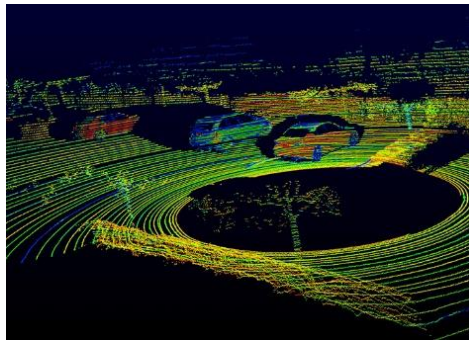


Figure 2-5 A picture of raw data from HDL-64E [20]

2.2 Triangulation Method

Figure 2-6 is a schematic diagram of the passive triangulation ranging method [21]. The distance between two observation points A, and B is D . Here the hypothetical situation is that the object is self-luminous, known as passive triangulation method. Active triangulation is to illuminate the measured object by using a laser, which will be discussed later.

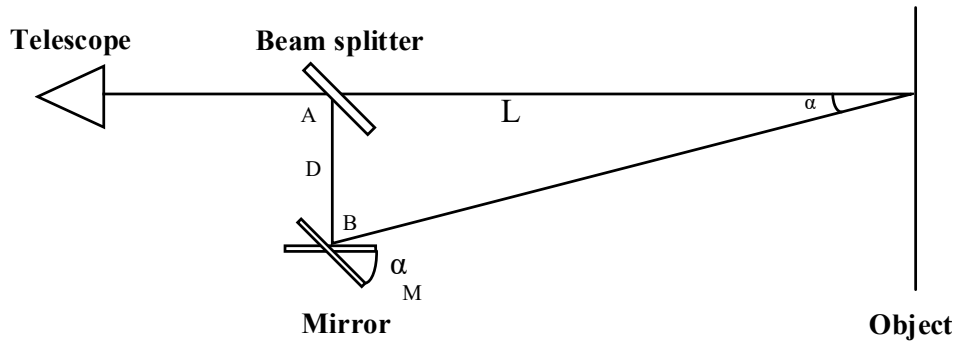


Figure 2-6 Conceptual image of the passive triangulation

Adjusting the beam splitter and turning the mirror M so that the points A and B coincide. Mirror M rotates from the initial angle $\alpha = 0$ (parallel to the beam splitter) to an angle, and then the telescope can see the objects coincide. The measured distance is shown in Eq. (2.1):

$$L = D/\tan(\alpha) \approx D/\alpha \quad (2.1)$$

As can be seen from Eq. (2.1), the approach requires to accurately measure the tiny angle α and the short baseline D to determine the ranging distance L.

The active optical rangefinder adds a light source and a position sensor to detect the reflected light to improve the performance. Removing the rotating parts can get a faster response. The structure of this instruments varies according to the actual demand of the application. Figure 2-7 is an active optical rangefinder for short distances (measuring ranges from 1 to 10 m). It equips a semiconductor laser and a Charge-Coupled Device (CCD). The eyepiece is a telescope with a focal length F_{rec} (typically 250 mm). The CCD is a device made of silicon and is linearly arranged by N separate photosensitive units. The width of each unit is ω_{CCD} (typical N = 1024, $\omega_{CCD} = 10 \mu\text{m}$). The spot of the object is imaged on the CCD by the objective lens. It is easy to calculate the resolution of the angle: $\Delta\alpha = \omega_{CCD}/F_{rec} = 0.04 \text{ mrad}$. For D = 50 mm, the actual accuracy of ranging distance L = 1 m is around 1 mm.

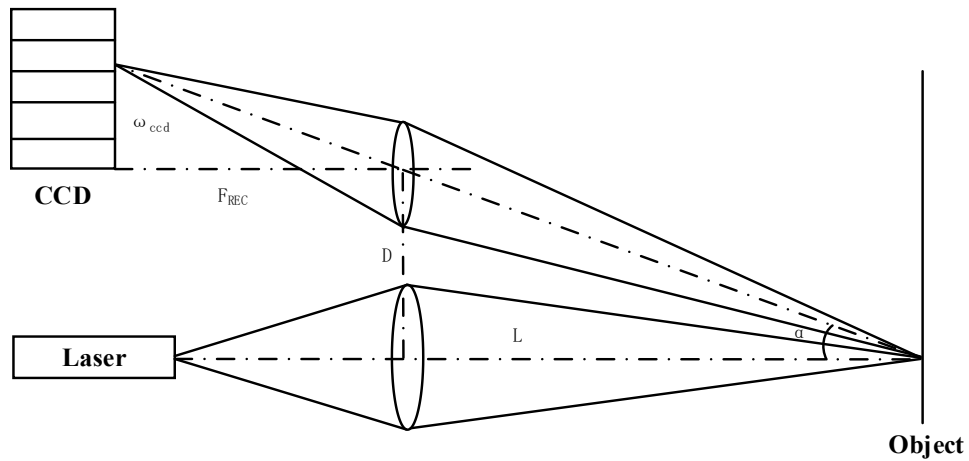


Figure 2-7 Conceptual image of the active triangulation

Through the above principle and precision analysis, the triangulation laser ranging method cannot achieve a high-precision and long-distance measurement. As the measurement distance increases, the ranging error will increase significantly.

2.3 Interference Method

Laser interference method is a classical precision ranging method. Laser interferometry calculates the distance by moving the measured object and detecting the coherent light. The increment of ranging length is obtained by measuring the number of $\lambda/2$ where λ is the wavelength of the laser. The sensitivity of the interference method can reach the nanoscale. According to the principle of light interference, the two beams with a fixed phase difference, the same frequency, the same vibration direction or tiny different vibration direction overlap each other to produce interference [22].

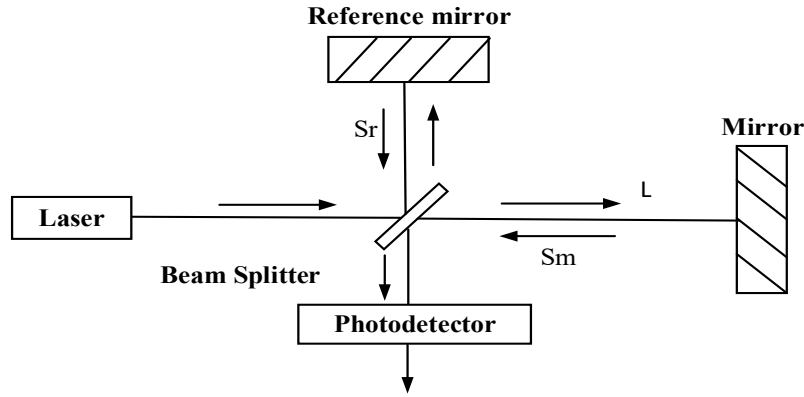


Figure 2-8 Conceptual image of the interference method

Figure 2-8 shows the conceptual image of the commonly used Michelson interferometer. This interferometer operates the laser as the light source, the measurement mirror in the position L can reach the resolution of $\lambda/2$. The beam emitted by the laser is divided into the reflected beam S_r and the transmitted beam S_m through the beam splitter. The two beams are reflected by a reference mirror and a measurement mirror, both two reflected beams are converged at a beam splitter into a coherent beam. The distance difference between the two reflected beams of S_r and S_m is L . When two light beams are superimposed, the intensity of resultant light is,

$$I = I_r + I_m + 2\sqrt{I_r I_m} \cos\left(\frac{2\pi L}{\lambda}\right) \quad (2.2)$$

where λ is the wavelength of the laser. When $L = N\lambda$, the phase difference of the two reflected beams is an integral multiple of 2π . The amplitude of the superimposed signal is increased which I is the largest, and the bright stripe appears. When $L = N\lambda + \frac{1}{2}\lambda$, the phase difference of the two beams is opposite. The amplitude of the two beams is offset which I is smallest, and the dark stripe appears. The two beams are then reflected by the beam splitter to the photodetector, the output signal is related to the brightness of the superimposed light. Assuming the beginning of the mirror spacing is L , and then the measurement mirror is moved along the direction of light forward. Each movement is an integral multiple of $\lambda/2$, the phase relationship of two beams changes from the same to the opposite. There is a bright and dim light alternately during one cycle and the output signal of the detector also changes once. The moving distance of the mirror $\Delta L = n\lambda/2$ can be determined from the number of the output signal changes. In the measurement, when the mirror

object is moving, to avoid recording the cosine signal, the linearity of movement must be guaranteed strictly which is difficult to achieve in practical applications.

As the wavelength of light is extremely short, especially the monochromatic nature of the laser, the wavelength value is very accurate. So, the resolution of the interferometric method can be at least $2/\lambda$, and the accuracy is micron level. The use of modern electronic technology is capable of measuring 0.01 optical interference fringes. Hence, the accuracy of the interference method ranging is extremely high, which is unmatched by any other ranging method.

With the development of technology and science, laser interference technology has continuously been developed. Also, besides the distance calculation, it can also achieve speed, angle, flatness, straightness, vertical and other parameters of the measurement. For example, the HP5529A interferometer manufactured by Hewlett-Packard company can make measuring the speed of 0.7 m/s. In the range of 40 m, the measurement resolution can reach 1 nm. Zygo also has its mature products, such as ZMI2000 interferometer, its measurement speed of 4.2 m/s. Within the measurement range of ± 21.2 m, the ranging resolution can achieve 0.62 nm and measuring acceleration range is 100 g (980 m/s). In the high precision and rapid measurement of the laser interferometer, the nonlinearity error in the laser interferometer and the Doppler shift generated during the mirror movement are the main factors that limit the ranging veracity of the laser interferometer. Many scholars on the above issues in-depth study and achieve initial results [23][24].

For the laser interferometric distance measurement approach, the measurement range is limited. It is mainly applied to short-range and high-precision measurements. To achieve the ranging procedure, it is necessary to ensure that the measuring beam is uninterrupted during the measurement process, and most of the precision guide rails are required. There are several measuring occasions in the industrial field do not possess the conditions of the guide rails, so that the use of the interference measurement method has been limited to a certain extent.

2.4 Frequency Modulation Continuous Wave

The principle of frequency modulation continuous wave (FMCW) ranging system is shown in Figure 2-9. The voltage-controlled oscillator (VCO) is controlled by the periodic linear

frequency scanning module to pass through the amplifier to the laser so that the frequency of emitted beam $f_e(t)$ is linearly changed. The period or time width of the light wave is much greater than the echo delay corresponding to the maximum range. The modulated laser beam is reflected by the target and then returned to the receiving part. After being received by the optoelectronic device, it is filtered and amplified and then mixed with $f_e(t)$ and filtered to obtain the difference frequency signal. By processing the filtered signal, the distance can be obtained.

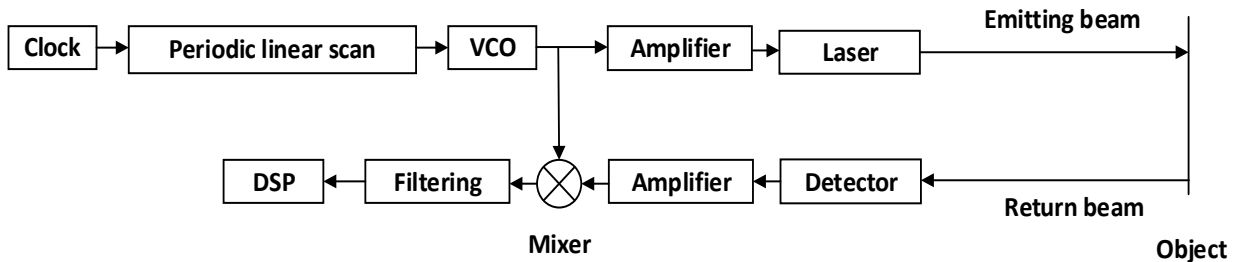


Figure 2-9 Conceptual image of the FMCW method

The relationship between beat frequency and time in FMCW ranging system is shown in Figure 2-10. The beat frequency signal acquired by mixing the echo signal $f_r(t)$ and $f_e(t)$ is $\Delta f = 2B \times (2R)/(cT)$, where B is the bandwidth of the transmitted signal, T is the modulation period of the transmitted signal, c is the speed of light, and R is the distance to be measured.

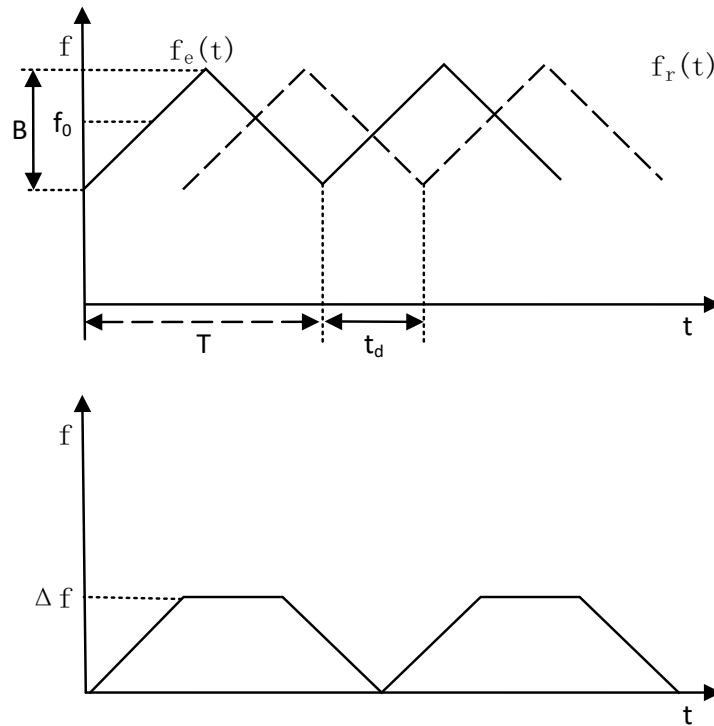


Figure 2-10 Relation between beat frequency and time in the FMCW method

Since the 1980s, the research work on FMCW laser ranging system has received universal attention. With the advancement of the hardware, the theoretical and technical level of FMCW ranging method has developed rapidly. In 1996, G.bazin and B.Journet used this conception to build a laser ranging system. The semiconductor laser is selected as the light source with a wavelength of 670 nm with the transmission power of 3 dBm. The frequency of the difference signal is 42MHz, and the measurement range is 2 meters to 50 meters [25]. In 2000, the experimental precision of the laser ranging device was better than 5 cm in the range of 40 meters reported from [26]. In 2001, D. Dupuy proposed the FMCW ranging method based on delay line technology. To solve the problem that the receiver and subsequent circuits receive a large amount of noise when receiving weak and wide-band echo signals, the APD is proposed as the photoelectricity receiver to enhance the signal-to-noise ratio [27]. World's first FMCW LiDAR for automotive applications from Blackmore has recently received a BMW investment with a maximum detection range of over 200m, speed measurements of $\pm 150\text{m/s}$ and resolution of 0.2m/s [28].

The primary advantages of FMCW ranging method are no distance blind zone, high resolution, low radiation power, simultaneous distance and speed measurement, and relatively simple equipment. However, this method is greatly influenced by the frequency stability and linearity of the transmitted signal. Even with various high-quality compensation methods, it is difficult for the VCO to have a linearity of 200 ppm. In the practical application environment, the presence of various interference sources also affects its measurement accuracy.

2.5 Time-of-Flight Method

Time of flight (TOF) method is a conventional distance measurement method, and there are already some broad-range applications such as terrain measurement, tactical ranging, missile trajectory tracking, and satellite, earth-to-lunar distance measurement [29]. Time of flight method uses the pulse laser with a high instantaneous power (up to a megawatt), short duration and relatively concentrated energy to measure the distance. For a cooperative target, the pulse laser ranging can reach a far range. For a non-cooperative target, ranging process can still be achieved by receiving the pulsed beam that is diffusely reflected from the target. The conceptual image of TOF method is shown in Figure 2-11.

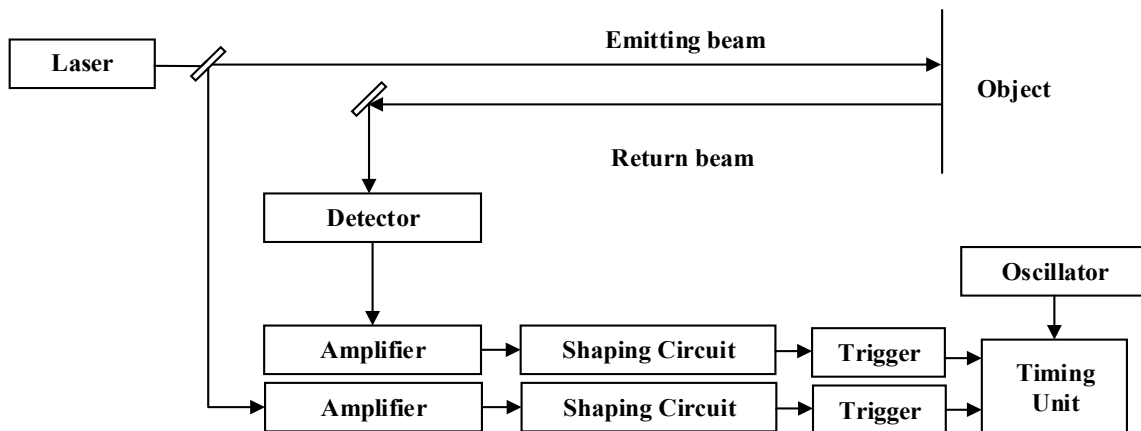


Figure 2-11 Conceptual image of TOF

The laser emits a pulse beam of high peak power, and a small portion of the energy of the pulse directly reaches the photodetection circuit through the internal optical system. This signal is a reference signal and serves as a starting point for the timing unit. Most of the energy of the optical

pulse is emitted to the target to be measured. After the laser pulse is reflected by the measured target, it is received by the photodetector circuit which is called the echo signal. The reference signal and the echo signal are successively converted into electrical pulses by the photodetector and then amplified and shaped. The shaped reference signal is used as the gate signal of the time interval measurement module to make it start timing. The shaped echo signal is adopted to turn off the interval measurement module to stop it from timing. The output of the time interval measurement module is the flight time between the laser transmitting and receiving. The ranging distance L can be calculated in equation (2.3),

$$L = \frac{c}{2} t \quad (2.3)$$

where c is the speed of light, t is the time interval.

2.5.1 Time Discrimination Method

By introducing the principle of pulsed laser ranging, to boost the measurement accuracy of the TOF laser ranging system, the time discrimination accuracy must be improved. The time t in equation (2.3) is the time difference between the transmitting time and the receiving time which is measured by the time discrimination system. If the time discrimination accuracy cannot be guaranteed, the laser flight time cannot be measured regardless of the accuracy of the subsequent time interval measurement system. Therefore, the correctness of the time discrimination is crucial.

There are two main time discrimination methods in TOF method: leading edge discriminator (LED) and constant fraction discriminator (CFD) [30].

The LED method is shown in Figure 2-12. The threshold voltage V_{th} is set to eliminate the jitter caused by the superposition of noise and echo signals. The voltage of the pulse signal is compared with the set threshold voltage. This operation is performed by a high-speed comparator. When the voltage intensity at a point on the leading edge of the pulse signal reaches the set threshold, this point is defined as the arrival time of the pulse signal.

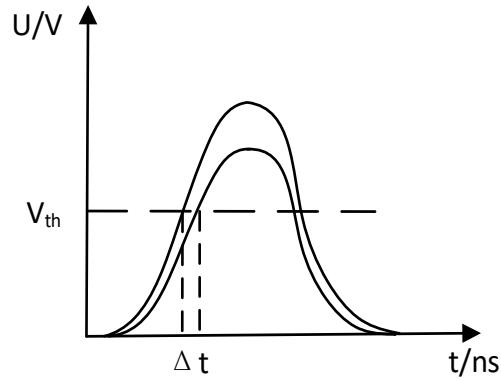


Figure 2-12 Leading edge discriminator

In Figure 2-12, the timing error is Δt . This error is significant and related to the shape of the pulse signal, the magnitude of the threshold voltage, the bandwidth of the receiving circuit, and the dynamic response. Therefore, the measurement accuracy of the LED method is hard to meet the requirement of high-precision laser ranging.

The CFD method is shown in Figure 2-13. The received pulse signal is processed through a series of circuits. When the amplitude of the signal comes to a certain proportion of the peak value, the position is the time when the pulse signal arrives. In Figure 2-13, the set ratio is 50% and the triggering time is at the half-maximum of the rising edge of the pulse signal.

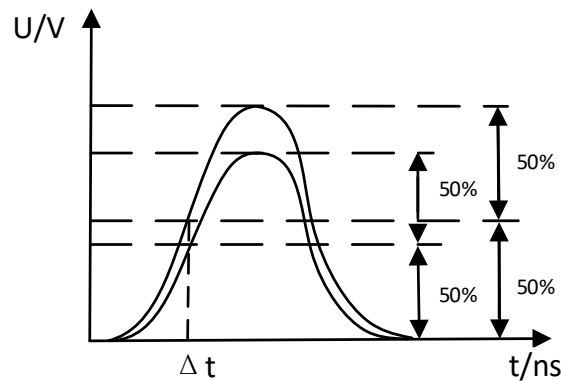


Figure 2-13 Constant fraction discriminator

Since the triggering time is not determined by a fixed threshold, this discrimination method is not affected by the magnitude of the amplitude. Even if the amplitude of the signal changes, it

will not generate too much time drift. Thus, the time error Δt caused by the variation of the amplitude and waveform of the signal is reduced at the CFD method.

To compensate for the timing error, sorts of gain control circuits are discussed in the previous papers [31][32]. By measuring the pulse width of the received signal and using the known relationship between the pulse width and the timing error, the timing error caused by the received pulse signal is reduced in [33]. Multiple thresholds method is proposed in [34][35] to minimize the timing error.

2.5.2 Time Interval Measurement Method

There are three commonly used time interval measurement methods: analog method, digital method, digital insertion method [30][32][36].

The analog method is to charge a known capacitor at a large current i_2 within the time interval to be measured t , and then discharge it with a small current i_1 . The discharge time is $\frac{i_1}{i_2} t$. The original time interval is expanded by $\frac{i_1}{i_2}$ times and greatly improved measurement accuracy. The advantage of this method is that the measurement accuracy can reach the order of picoseconds [37]. However, because of the non-linearity relationship between charge and discharge, the value of the measurement error caused by the non-linearity is 1/10000 of the measured distance, which limits the measurement range and measurement accuracy. Moreover, the charge and discharge performance of the capacitor is affected by the temperature ($10 \sim 30ps/^\circ C$). To achieve a higher measurement accuracy, a strict requirement of ambient temperature is needed [38].

The digital method, also known as a direct counter method, uses the counting pulses generated by the clock oscillator to measure the time interval. The error is one cycle of the clock oscillator. The time interval measurement error of the digital method mainly comes from the time difference between the rising edge of the clock oscillator and the rising edge of the start and stop pulses. If the time difference between the rising edge of the clock oscillator and the starting rising edge is denoted by t_1 and the time difference between the rising edge of the stop pulse is denoted as t_2 , the error of the time measurement is $\Delta T = t_2 - t_1$. Assuming that the resolution of the distance is required to be $P_L = 1m$, the frequency of the clock oscillator is required to be $150MHz$.

Even with a clock oscillator with a frequency of $10GHz$, the ranging accuracy is only $\pm 1cm$ and the high frequency requiring a wide bandwidth of the circuit which makes the circuit is difficult to be designed. Furthermore, the frequency of the clock oscillator cannot be increased without limitation, the resolution of the pulse range finder is generally low.

To accurately measure this time interval error's value, there is a digital insertion method. According to the different measurement methods, digital insertion method is divided into delay line insertion method, analog insertion method and differential frequency measurement insertion method [39][40][41]. The delay line insertion method obtains the value of t_1 and t_2 by the gate delay. The accuracy of the measurement depends on the delay time of the single gate delay, normally can reach the order of the hundred picoseconds, the corresponding ranging accuracy is the decimation level. Increasing the number of delay units will improve the accuracy of the corresponding ranging, but at the same time enhance the ranging blind spots. Analog insertion method has the similar way to obtain the ΔT with the above analog method by charging and discharging to widen the measured time. The method also exists time-extended non-linear error which limits its application. Differential frequency measurement insertion method uses the beat frequency signals generated by the reference signal and two signals with the same frequency and different phase to measure the broaden time. If the frequency of the clock signal is $f = 100MHz$, the frequency of reference signal is $F = 100MHz + 100KHz$, then the resolution is $(F - f)/Ff = 1ps$, the corresponding cut-off time is $1/(F - f) = 10\mu s$, and the measurement range is $1.5km$. The measurement accuracy of the differential frequency measurement method is higher than the other two methods, but it has high requirements for the accurate positioning of the starting signal and frequency stability. Furthermore, the blind spot is large, thus it cannot meet the application of long-distance and high-precision measurement occasions.

The measurement correctness of the pulse laser ranging is also related to the rise time and duration (i.e., pulse width) of the laser pulse, the bandwidth of the laser receiving system, the degree of the laser beam being widened by the target. When the laser pulse is not the ideal pulse signal, the emission pulse is narrower, and the front edge of the pulse is steeper, the higher accuracy of ranging can be achieved. At present, the pulse width of the mode-locked laser minimum can reach $10^{-18}S$, the peak power is more than $10^{12}W$, which provides the possibility of further improvement in the measurement accuracy of the TOF laser ranging method. To improve the

accuracy of ranging, a steep pulse front edge is needed, and a sufficient bandwidth of the receiver is required, the current bandwidth of photodetector is $1\text{GHz} \sim 4\text{GHz}$ [42][43]. The development of the complementary metal-oxide-semiconductor (CMOS) fabrication process allows the bandwidth of the subsequent amplifying circuit to be between 50MHz and 500MHz [44][45]. However, increasing the bandwidth of the receiver will reduce the signal to noise ratio of receiving system. Considering all aspects, the bandwidth of the receiver is below 100MHz , and the response speed will cause pulse broadening. If the pulse broadening is 3.3ns , the corresponding ranging error is 1m . In addition, the accuracy of the TOF laser ranging method is also affected by atmospheric attenuation, target reflection characteristics and subsequent circuits.

2.5.3 Applications of Time-of-Flight Method

TOF laser ranging method has the features of long-range, lightweight, simple structure widely used in military, aerospace and other fields. In 1973 the NASA, United States installed a rangefinder in the SKYLAB satellite, the rangefinder has a measuring range of 453Km , ranging accuracy of 15m [46]. In 1985, the Five-Year Plan of United States Navy's GEODetic Satellite (GEOSAT) using the ALT LIDAR to further reduce the noise effects, demonstrated the tremendous potential for pulse laser ranging. In 1995, their ERS-2 program, the satellite orbit measurement accuracy was 0.5m . To 1997, In JGM3, the satellite orbit measurement accuracy has reached 10cm [47][48][49]. On November 25, 2011, the LIDAR system of Mars Rover launched by the Mars Science Laboratory played a significant role in the safety and accuracy of detection during of MARS detection. During the detector's descent, the ranging range of equipped LIDAR is less than 10km . In civilian fields, the pulse laser equipped on the Velodyne's VLP-16 LIDAR sensor can reach an accuracy of $\pm 3\text{cm}$ within the range of 100m which can be applied for not only for autonomous vehicles but also many other applications.

At present, the pulse laser rangefinder has a wide range of applications, whether it is long-distance measurement or portable short-range ranging. Typically, the pulse laser ranging can achieve rapid long-range measurement, but the absolute measurement accuracy is not precise.

2.6 Phase-Shift Method

The phase-shift laser ranging method calculates the phase difference between the transmitted signal and reference signal to get the ranging distance. The conceptual image of the phase-shift method is shown in Figure 2-14 [50].

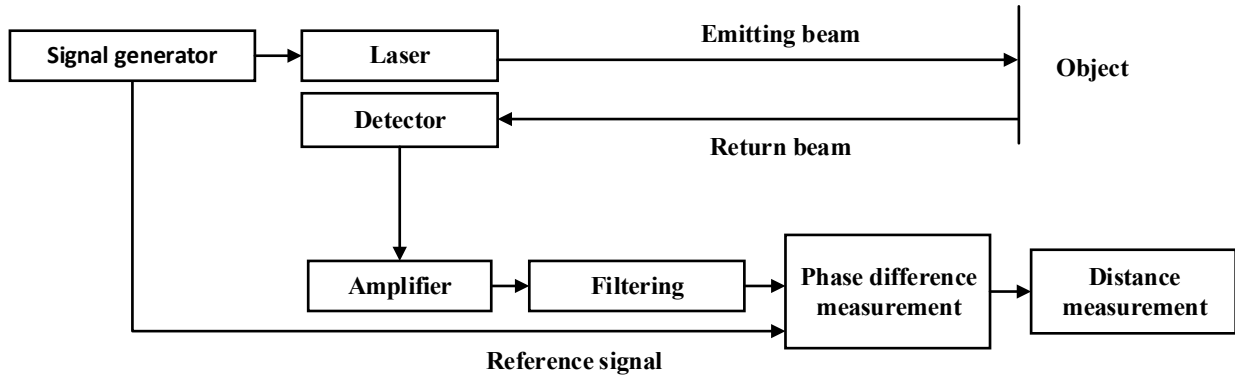


Figure 2-14 Conceptual image of the phase-shift method

The signal generator drives the laser to emit the sinusoidally modulated light, which is reflected by the object and received by the detector. Then the received signal is amplified and filtered. The phase difference measurement unit calculates the phase difference between the received signal and the reference signal. Then according to the phase difference, the measured distance is obtained. Assuming phase difference is $\Delta\varphi$, the ranging distance can be expressed as,

$$L = \frac{1}{2} ct = c \frac{\Delta\varphi}{4\pi f} \quad (2.4)$$

where c is the speed of light, f is the modulation frequency.

2.6.1 Phase-Shift Measurement Method

By analyzing the principle of the phase-shift method, the accuracy of the distance measurement is determined by the precision of the phase-shift measurement. The traditional phase measurement method has analog phase identification [51], automatic digital phase identification [52] and a combination of these two methods [53]. The above methods are carried out in the time domain and require a higher signal-to-noise ratio, and cannot separate multiple received signals.

Moreover, the above method is influenced by the amplitude-phase error in the phase measurement. To reduce the amplitude-phase error, the sophisticated control circuit is often used to adjust the amplitude of the received signal, which increases the complexity of the circuit and prolongs the measurement time.

In recent years, the phase measurement method gradually goes to the digital direction. The advantages of the digital method are: low hardware costs, and adaptability. Also, the accuracy of the digital method is higher than the analog measurement. From 1996 to 1998, B. Journet and his team designed a phase-shift laser ranging system by using automatic digital phase demodulation to measure the phase difference [54][55]. By 2001, the phase measurement method based on the four-quadrant sampling technique also called digital synchronous detection increased the phase measurement accuracy from the original 27° to 0.02° [56][57]. This shows the great advantages of digital processing technology. Since then, digital synchronous detection has been widely used in phase-shift laser ranging [58][59]. Afterward, to avoid the use of high sampling frequency, a laser rangefinder system with under-sampling technique and digital synchronous detection are proposed in [60]. J. F. Munro introduced the Discrete Fourier Transform (DFT) method to the phase measurement. Four-point DFT sampled in one cycle of the reference signal and received signal was used to compute the corresponding phase of the fundamental waves. The phase difference between the two signals can be calculated. Since then, numerous applications of DFT and Fast Fourier Transform (FFT) in the phase-shift laser ranging method have been studied [61].

2.6.2 Multi-Value Problem of Phase-Shift Ranging System

The distance calculation of phase-shift laser ranging system is achieved by modulating the frequency of light and measuring the phase shift $\Delta\varphi$ of the modulated laser signal formed on the distance L . The propagation time t between the measurement point and the target is measured indirectly. Eventually, according to the speed of light, the distance L can be measured.

Figure 2-15 shows the modulated optical signal propagates in the phase-shift laser ranging system. The light wave is transmitted from point A to the object B and eventually received at point C .

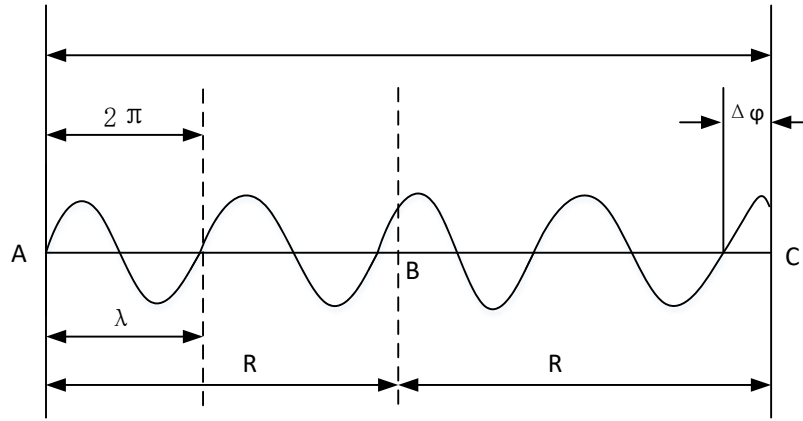


Figure 2-15 Principle of the modulated laser propagating on the measured distance

Supposing the modulation frequency is f , the wavelength $\lambda = \frac{c}{f}$ and c is the speed of light.

The phase shift from the point A to the point C can be expressed as,

$$\varphi = 2m\pi + \Delta\varphi = 2\pi \left(m + \frac{\Delta\varphi}{2\pi} \right), m = 0, 1, 2 \dots \quad (2.5)$$

where m is the number of integer period. Let the time from point A to point C is t , the distance L between A and B can be obtained in equation (2.6).

$$L = \frac{1}{2} ct = c \frac{\varphi}{4\pi f} = \frac{1}{2} \lambda \left(m + \frac{\Delta\varphi}{2\pi} \right) \quad (2.6)$$

The maximum measurable distance in the phase-shift laser ranging system is called the maximum non-ambiguity range (NAR). According to the modulation frequency f , the maximum NAR can be expressed as:

$$NAR_f = \frac{c}{2f} \quad (2.7)$$

From Eq. (2.7), the modulation frequency f determines the maximum measurable distance of the system. The maximum NAR decreases as the modulation frequency increases. Regarding the maximum measurable distance, equation (2.6) can be changed to:

$$L = \frac{1}{2}ct = \frac{c}{2f} \times \frac{\Delta\varphi}{2\pi} \quad (2.8)$$

The corresponding distance measurement error can be express as,

$$\Delta L = \frac{c}{2f} \times \frac{\delta\Delta\varphi}{2\pi} \quad (2.9)$$

where $\delta\Delta\varphi$ is the phase measuring accuracy.

For equation (2.9), as the precision of phase difference measurement is a constant, the ranging accuracy increases with the modulation frequency. According to Eq. (2.8) and Eq. (2.9), there is a contradiction between the maximum NAR and the ranging accuracy in the phase-shift laser ranging method.

To extend the measurement range and increase the ranging accuracy, the multiple-frequency measurement technology is proposed in the phase-shift laser ranging method. The primary principle is: using several beams with different modulation frequencies measure the same distance [62]. The highest frequency signal can be used to ensure measurement accuracy, and the lowest frequency signal can be used to ensure the measurement range. The multiple measurement results are combined to achieve high-accuracy and long-distance measurements. A phase-shift laser rangefinder based on two modulation frequencies is designed to achieve full range and high ranging resolution [60]. From 2012 to 2013, S. Hwang introduced a kind of polarity beam splitter (PBS) to overcome the disadvantage of the conventional electrical combination of two modulation signals [63][64]. By applying three digital signal processors and three direct digital synthesizers, multi-frequency modulation laser can be transmitted and received simultaneously [65]. In 2018, a coherent dual-frequency laser ranging system is designed and proposed in [66] where a 250 m ranging length and 0.1 m distance resolution ranging result is achieved. However, there is an issue that the modulation signal is easily distorted, and the modulation depth is low for continuous modulation of light intensity especially at high modulation frequencies, thereby limiting the measurement distance of the phase-shift laser ranging technology.

2.6.3 Applications of Phase-Shift Method

In the field of civil, the laser rangefinder is utilized for distance, area and volume measurement. In the mature laser ranging products, the measurement range of handheld rangefinder is less than 500m such as Leica A6, HILTI PD32, Dimetix DLS-A30. In some military applications, it's often required dynamic, high-precision ranging of moving targets, which raises some new requirements for distance measurement techniques. European Space Agency (ESA) began to develop space rendezvous radar and detector technology from the beginning of the 1980s. In 1985, Germany MBB company developed the independent laser rangefinder combined with the silicon CCD to complete the distance, speed and attitude measurement. In this system, for the measurement of distance and speed, the 10.6 μ m-wavelength carbon-dioxide laser is selected as the light source, the infrared detector is the receiver, and the measurement is realized by the CCD [67]. Japan launched the satellite EST-VII on November 28, 1997, and in July 1998 to August, it achieved rendezvous and other tasks. The distance measurement system diagram used in EST-VII is shown in Figure 2-16 [68].

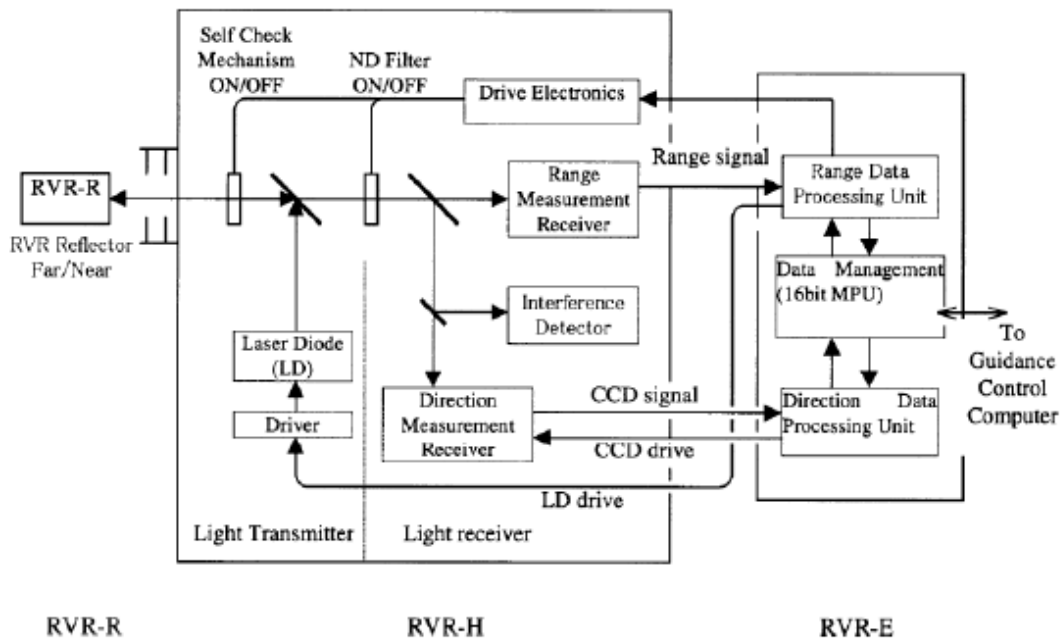


Figure 2-16 Diagram of ETS-VII distance measurement system [68]

In the final stage of the docking, the distance measurement method is mainly composed of the phase-shift laser ranging method and CCD. The measurement range is 0.3~600m, the remote-

end measurement accuracy is $1m$, and the near-end measurement accuracy is $10cm$. The emission system uses the method of light intensity modulation of the laser, the modulation frequencies are $15MHz$ and $14.55MHz$ respectively. In the receiving system, the receiving device is APD and the array CCD. The received light is divided into two beams, which are sent to the array CCD and APD respectively. The CCD detects the two-dimensional position information of the return light and calculates the aiming angle of the target. APD is used to detect optical power and target distance.

Currently, the phase-shift laser ranging method can measure the distance of tens of meters to several hundred meters, and measurement accuracy achieves the millimeter level.

2.7 Comparison of Laser Ranging Method

Through the description of the five kinds of laser ranging methods, each ranging method has its advantages and limitations. The research of laser ranging system is characterized by vast measurement distance and reliable precision.

Triangulation method is simple and has a fast ranging speed, but it does not apply high-precision ranging.

The accuracy of the interferometric method is sufficient to meet the precision requirement while it is only suitable for short distance ranging, the condition of the measurement environment is extremely demanding.

In theory, the maximum ranging length of FMCW method is determined by the modulation period of the transmitted signal. However, due to the limitation of the signal-to-noise ratio, the ranging range is generally below $200m$. Therefore, FMCW is not suitable for large-scale and high-precision ranging.

For TOF ranging method, the signal is attenuated and distorted to some degree during the propagation of the pulse laser signal. Even in the time discrimination unit, the shape and amplitude of the transmitted pulse signal and the received pulse signal have a specific difference which is hard to determine the starting and ending time accurately. Accordingly, the ranging accuracy of the pulse laser ranging method cannot reach to a high standard.

For the phase-shift method, it can achieve a high ranging accuracy in a specific range. Nonetheless, compared with the TOF method, the phase-shift method has more massive power consumption and distortion which cannot be used in the long-distance situation.

The classic ranging methods are compared in Table 2.1.

Table 2-1 Comparison of commonly used ranging methods

Distance measurement method	Range	Accuracy	Application
Triangulation method	Millimeter	Micron	Industrial: shape and position measurement
Interferometric method	Centimeter	Micron	Crustal deformation, continental, seismic volcanic forecast
FMCW method	Meters to hundred meters	Millimeters	Driverless
TOF method	Tens of meters to tens of thousands of kilometers	Meter	Military, scientific research
Phase-shift method	Meters to hundred meters	Millimeters	Engineering, sports measurement

2.8 Motivation and Contribution

Laser has high angular resolution and anti-interference ability which is widely used in the field of distance ranging. Currently, widely used laser ranging methods are TOF method and the phase-shift method. Compared with the TOF method, phase-shift laser ranging technology has a feature of high-frequency and high-precision measurement. However, to ensure the accuracy of the phase-shift method, the frequency of the laser modulation signal is about 100 megahertz which results in the measurement range of less than 2m under the single-frequency signal [69]. Furthermore, the problem of large power consumption and easily distortion for continuous signals should also be considered. Thus, the traditional phase-shift laser ranging system cannot meet the measurement requirements of considerable distance.

The TOF method and the phase-shift method are similar in principle by utilizing the propagating time of the laser beam to measure the distance. The difference between these two

methods lies in the use of timing circuit and phase difference measurement, respectively. It is not difficult to find that their advantages and limitations can be complementary. Few previous works have researched on merging the TOF method and the phase-shift method. Reference [70] introduces a novel structure that a pulse light with a repetition rate of 8.5 KHz is transmitted and then the phase difference is calculated from the undersampled data. Although the measurement range is up to 7000 m theoretically, the ranging accuracy is inferior because of the low transmitting frequency. Another work combines these two kinds of methods by sending multi-cycle sinusoidal signals with the modulation frequency $f = 10\text{MHz}$ [71]. The rough measurement is realized by the transmitting time, and the measurement precision is improved by the phase-shift between the emitted signal and reference signal. However, due to the high-power consumption and distortion of sinusoidal signals, this method cannot reach a long-ranging distance.

According to the Fourier Series of the pulse signal, it is possible to implement the phase difference calculation on the pulse laser ranging system to solve the contradiction between ranging distance and ranging accuracy. In this thesis, a systematic comparative analysis of the commonly used phase detection methods are analyzed under the influence of signal-to-noise ratio, frequency offset, and harmonic interference. Afterward, two kinds of hybrid pulse and phase-shift laser rangefinder systems are proposed. One of them is dual-frequency pulse laser ranging system, which utilizes low-frequency signal to get the position within a broad range and high-frequency signal to achieve an accurate measurement. Another method realizes coarse measurement and precise measurement of distance by measuring the time difference and phase difference in only one pulse signal which is called signal-frequency pulse laser ranging system. Finally, through establishing the co-simulation model of the above two ranging systems in OpiSystem and MATLAB, high-precision and long-distance ranging systems can be achieved.

Chapter 3 Analysis and Design of Hybrid Pulse and Phase-Shift Laser Ranging System

In this chapter, the characteristics and critical problems of the pulse laser and phase-shift laser ranging systems are introduced and analyzed. To eliminate the contradiction between the unambiguous range and the measurement precision in the phase-shift laser ranging system, based on the advantages of the two ranging technologies, two hybrid pulse and phase-shift laser ranging methods are proposed. After that, the schemes of two ranging systems are analyzed, and the selected frequency of the transmitting pulse signal was discussed.

3.1 Combination of Pulse Method and Phase-Shift Method

In the conventional phase-shift laser ranging technology, the intensity modulation of the laser is performed by using a continuous modulation signal, and the direct intensity modulation of the semiconductor laser causes the laser to operate in a continuous state. The continuous operation of the laser not only consumes power but also reduces the lifetime of the laser. Also, the sinusoidal waveform is easily deformed, and the measurement distance is limited. According to the analysis, the idea of converting a continuous modulated signal into a pulse modulated signal to modulate the laser is generated. The modulated pulse signal can also be able to reflect the phase information of the continuous modulated signal. By transmitting the pulse signal, the power consumption can be reduced, the lifetime of the laser can be extended, and the contradiction between the measurement distance and the ranging accuracy in the phase-shift distance measurement can also be solved. The characteristic of the pulse signal will be discussed later.

3.1.1 Fourier Series of Pulse Signal

The periodic pulse signal in the time domain can be express as,

$$f(t) = \begin{cases} E, & nT_1 - \frac{\tau}{2} \leq t \leq nT_1 + \frac{\tau}{2} \\ 0, & \text{otherwise} \end{cases} \quad n = 0,1,2,3 \dots \dots \quad (3.1)$$

where E is the amplitude, T_1 is the period of signal and τ is pulse width. Using Fourier Series expansion, the above pulse signal can be rewritten as an infinite sum of sinusoidal waves [72],

$$f(t) = \frac{a_0}{2} + \sum_{k=1}^{\infty} (a_k \cos(2k\pi ft) + b_k \sin(2k\pi ft)) \quad (3.2)$$

where the f is the frequency of the signal. Since the signal function in equation (3.1) is even, it can be simplified as,

$$f(t) = \frac{a_0}{2} + \sum_{k=1}^{\infty} (a_k \cos(2k\pi ft)) \quad (3.2)$$

where $\frac{a_0}{2}$ can be expressed as,

$$\frac{a_0}{2} = E \frac{\tau}{T} \quad (3.4)$$

Since the periodic pulse signal $f(t) = E$ from $-\frac{\tau}{2}$ to $+\frac{\tau}{2}$ and $f(t) = 0$ elsewhere in one period, the other a_k can be solved as,

$$\begin{aligned} a_k &= \int_T f(t) \cos(2k\pi ft) dt, k \neq 0 \\ &= \frac{2}{T} \int_{-\frac{T}{2}}^{\frac{T}{2}} f(t) \cos(2k\pi ft) dt \\ &= \frac{2}{T} \int_{-\frac{\tau}{2}}^{\frac{\tau}{2}} E \cos(2k\pi ft) dt \\ &= \frac{2}{T} \frac{E}{2k\pi f} \sin(2k\pi ft) \Big|_{-\frac{\tau}{2}}^{+\frac{\tau}{2}} \end{aligned}$$

$$= \frac{1}{T} \frac{E}{k\pi f} (\sin(k\pi f\tau) - \sin(-2k\pi f\tau)) \quad (3.5)$$

As the fact that $f = \frac{1}{T}$ and sine signal is an odd function, $\sin(\alpha) - \sin(-\alpha) = 2 \sin(\alpha)$, it can be simplified as,

$$a_k = \frac{2}{T} \frac{E}{k\pi f} \sin(k\pi f\tau) = \frac{2E}{k\pi} \sin(k\pi f\tau) \quad (3.6)$$

The expression of $f(t)$ can be expressed as,

$$f(t) = E \frac{\tau}{T} + \sum_{k=1}^{\infty} \left(\frac{2E}{k\pi} \sin(k\pi f\tau) \cos(2k\pi f t) \right) \quad (3.7)$$

As can be seen, the periodic pulse signal always contains the components of integer harmonic frequencies which is independent of the duty cycle.

For the exponential Fourier Series, the function of the periodic pulse signal is expressed as,

$$f(t) = \sum_{n=-\infty}^{\infty} C_n e^{jn\omega_0 t} \quad (3.8)$$

where C_n is called the exponential Fourier Series coefficients. By using Euler's formula, the coefficients C_n are given in (3.9).

$$\begin{aligned} C_n &= \frac{1}{T} \int_{-\frac{\tau}{2}}^{+\frac{\tau}{2}} f(t) e^{-jn\omega_0 t} dt = \frac{1}{T} \int_{-\frac{\tau}{2}}^{+\frac{\tau}{2}} f(t) e^{-jn\omega_0 t} dt \\ &= \frac{E}{-jn\omega_0 T} \left(e^{-jn\omega_0 \frac{\tau}{2}} - e^{+jn\omega_0 \frac{\tau}{2}} \right) = \frac{E}{-jn2\pi} \left(e^{-jn\frac{\pi\tau}{T}} - e^{+jn\frac{\pi\tau}{T}} \right) \\ &= \frac{E}{-jn2\pi} 2j \sin\left(-n\frac{\pi\tau}{T}\right) = \frac{E}{n\pi} \sin\left(n\frac{\pi\tau}{T}\right) \end{aligned}$$

$$\begin{aligned}
 &= \frac{E}{T} \frac{\sin\left(\frac{n\pi\tau}{T}\right)}{\frac{n\pi\tau}{T}} \\
 &= \frac{E\tau}{T} \operatorname{sinc}\left(\frac{n\pi\tau}{T}\right)
 \end{aligned} \tag{3.9}$$

Now considering the case, E and τ are fixed where $E = 1, \tau = \frac{1}{20} \text{ s}$. Period T is $T_1 = \frac{1}{4} \text{ s}$ and $T_2 = \frac{1}{2} \text{ s}$ respectively. The figures of periodic pulse signal $f(t)$ and Fourier Series coefficients C_n are shown in Figure 3-1 and Figure 3-2.

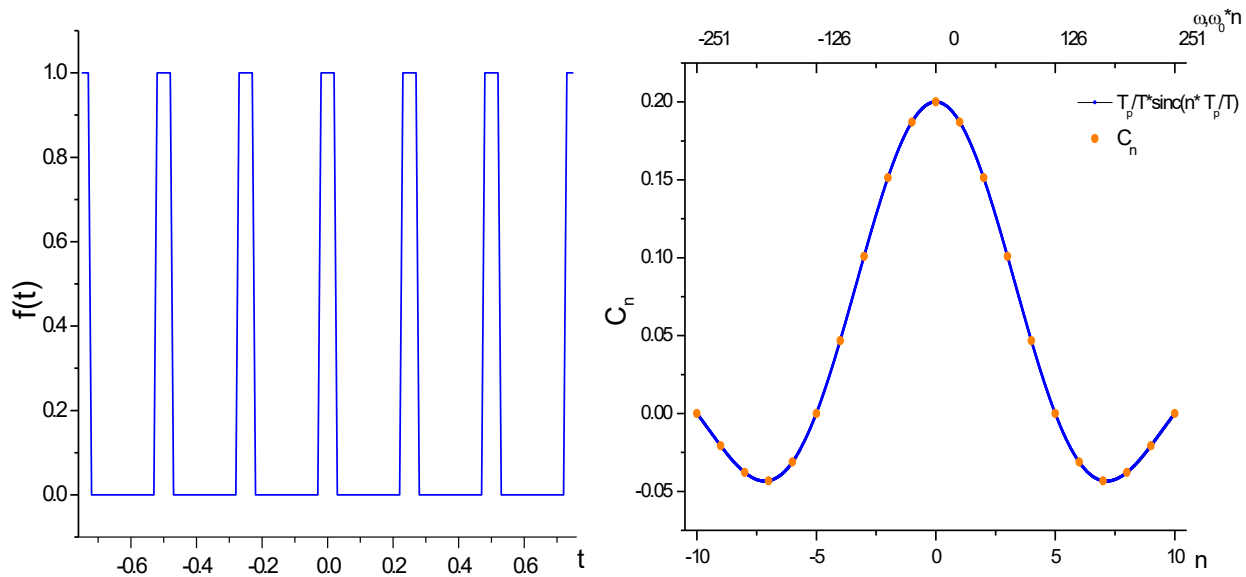


Figure 3-1 Pulse signal $f(t)$ and Fourier Series coefficients C_n when $\tau_1 = \frac{1}{20} \text{ s}, T_1 = \frac{1}{4} \text{ s}$

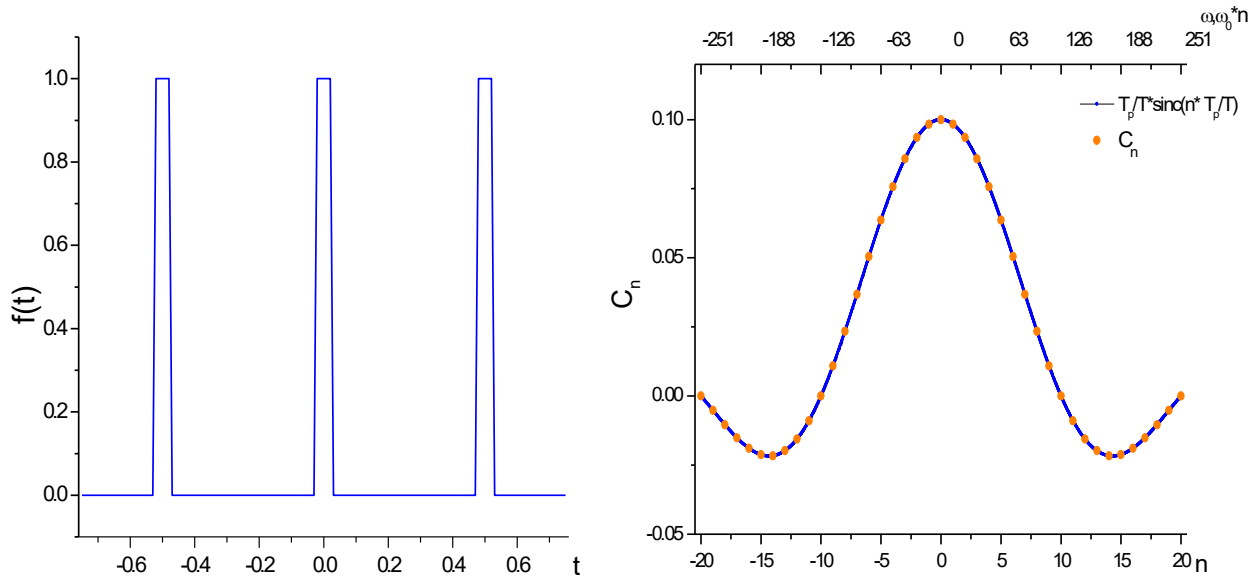


Figure 3-2 Pulse signal $f(t)$ and Fourier Series coefficients C_n when $\tau_2 = \frac{1}{20} s$, $T_2 = \frac{1}{2} s$

The image on the left side of the figure shows the periodic pulse signal $f(t)$ in the time domain and the graph of Fourier Series coefficients C_n is displayed on the right side. As can be seen from Figure 3-1 and Figure 3-2, the Fourier Series coefficients are discrete, harmonic, and convergent. For the right side of the figure, there are two scales used on the horizontal axis. On the bottom side, the scale is the integer index n . On the top side, it shows the frequency ω determined by $\omega = \omega_0 * n$ where $\omega_0 = \frac{2\pi}{T}$ and T is the period of the signal $f(t)$. Thus, the spacing between two points is ω_0 and $\omega_0 \times n$ is the n^{th} harmonic. As T increases, ω_0 decreases, therefore, the amplitude of C_n decreases, the spacing between two points becomes smaller and effective harmonic components increase.

Now assuming E and T are fixed where $E = 1$, $T = \frac{1}{2} s$. Pulse width τ is set to $\frac{1}{20} s$ and $\frac{1}{8} s$ respectively. The figures of periodic pulse signal $f(t)$ and Fourier Series coefficients C_n when are shown in Figure 3-3.

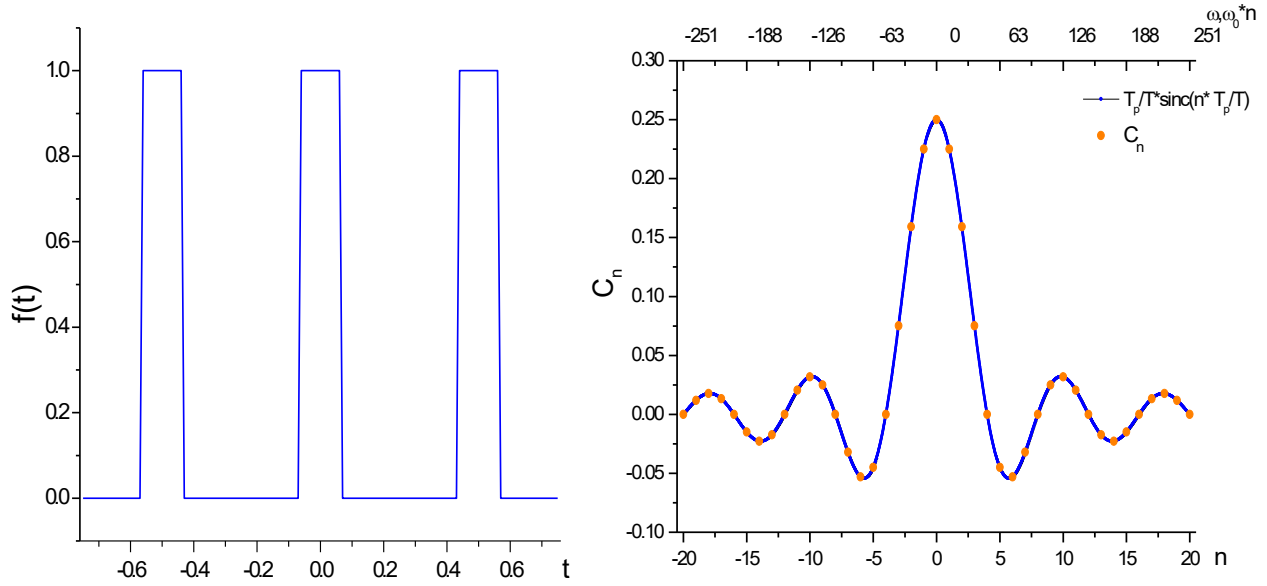


Figure 3-3 Pulse signal $f(t)$ and Fourier Series coefficients C_n when $\tau_3 = \frac{1}{8} s$, $T_3 = \frac{1}{2} s$

Compared with Figure 3-2 and Figure 3-3, as the pulse width τ increases in the time domain, Fourier Series coefficients C_n becomes more localized, the amplitude of C_n increases, the spacing between two points unchanged and effective harmonic components reduce.

As can be seen from the above analysis that the periodic pulse signal is composed of an infinite sum of discrete spectral components. For a single-frequency sine wave, after turning it into a pulse signal with the same frequency, the pulse signal also contains the former sinusoidal wave. As long as the frequency is filtered out through a low-pass filter or band-pass filter, the same frequency signal can be restored. Therefore, this principle can be used in the pulse laser distance measurement system to convert the transmitted pulse signal into a sinusoidal signal with the same frequency to realize phase difference measurement.

3.1.2 Heterodyne Detection Technology

When the laser modulation frequency is high, and the phase of the signal is measured directly, the complexity of circuit is increased which will affect the phase measurement correctness and reduce the accuracy of ranging [69]. Therefore, the heterodyne technology is needed in phase measurement. The principle of heterodyne detection technology is shown in Figure 3-4.

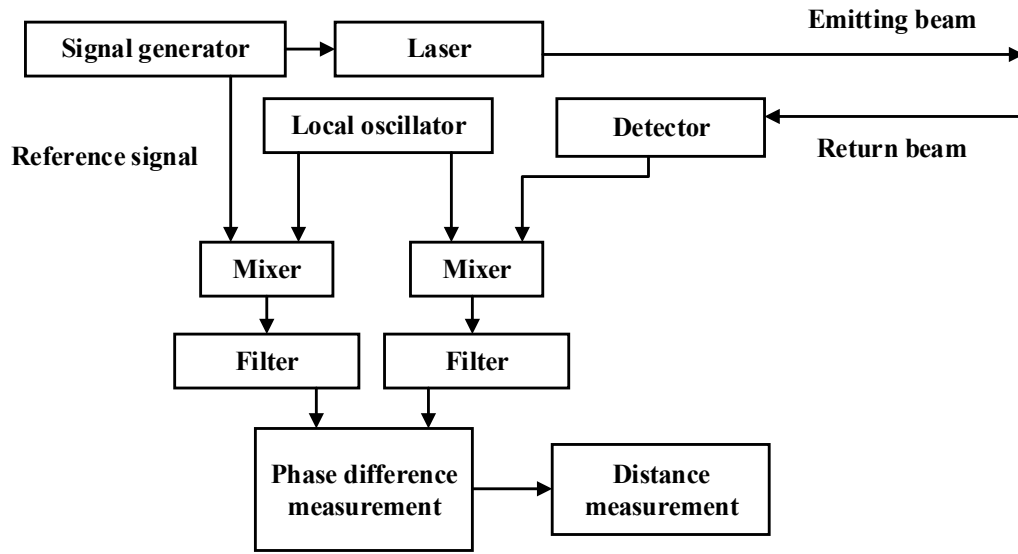


Figure 3-4 The principle of heterodyne detection technology

Both the reference signal and the received signal were mixed with the signal from the local oscillator. Through the low-pass filter, a low-frequency signal can be obtained from the mixed signal. The filtered signal is sent to the phase measurement unit which can reduce the circuit complexity and improve the ranging precision.

Supposing the signal after emitting unit as shown below,

$$E_e = A \cos(\omega_e t + \varphi_e) \quad (3.10)$$

The received signal can be expressed as,

$$E_r = B \cos(\omega_e t + \varphi_e + \Delta\varphi) \quad (3.11)$$

where $\Delta\varphi$ is the phase change in propagation.

The local oscillating signal is express as:

$$E_l = C \cos(\omega_l t + \varphi_l) \quad (3.12)$$

The low-frequency reference signal and the ranging signal are obtained at the output of the mixers, and express as:

$$D_r = D \cos[(\omega_e - \omega_1)t + (\varphi_e + \omega_1)] \quad (3.13)$$

$$D_s = D \cos[(\omega_e - \omega_1)t + (\varphi_e + \omega_1) + \Delta\varphi] \quad (3.14)$$

It can be seen from the above equations that the frequency of the signal can be reduced while preserving the phase information of the signal. The phase difference $\Delta\varphi$ between the two filtered signals is measured by the phase detection circuit. Normally, the frequency of the filtered signal is less than 100 KHz. Therefore, by using the heterodyne detection technology, the circuit complexity is reduced while increasing the ranging accuracy.

3.1.3 Beam Divergence

The light pulse signal will diffuse into a circle or an ellipse when it arrives at the object to be detected no matter how collimated it emits from the laser rangefinder. When the beam has a fixed spread angle, the farther it is emitted, the larger the diameter of the light illuminated on the measured object. Therefore, if the object has an irregular shape, the reflected pulse signal will be the average of the intensity of the illumination on the object. Figure 3-5 illustrates the geometric representation of the transmitting beam and reflected beam between the laser rangefinder and the object [73]. In Figure 3-5, θ is the divergence angle of the beam, d is the diameter of the laser rangefinder, and R is the measuring distance.

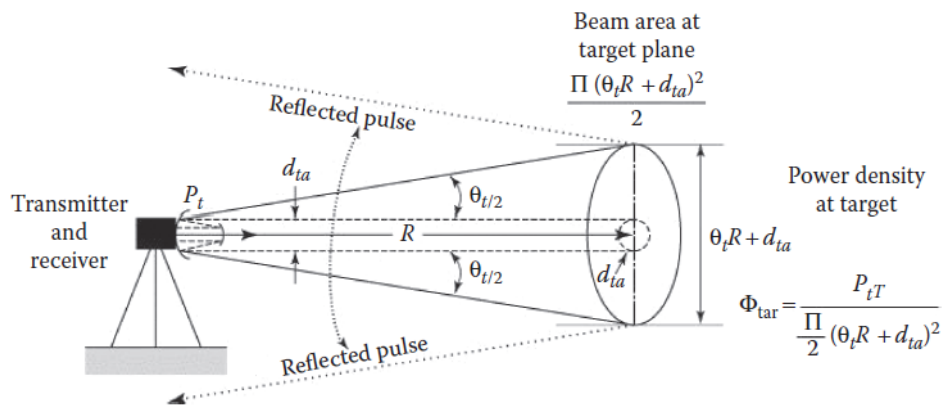


Figure 3-5 The geometric representation of the transmitting beam and reflected beam [73]

The book [74] provides further discussions on beam divergence in laser ranging field. The typical beam divergence value for the laser rangefinder is between 0.3 mrad and 2 mrad. For a ranging distance of 1000 meters, the beam diameter has an aperture of 30 cm as the beam divergence is 0.3 mrad.

3.1.4 Reflectivity

In the process of laser ranging, the reflectivity of the measured object has a significant influence on the ranging correctness. For the plane of an object, the ratio of incident light to reflected light is called reflectivity. Apparently, if the reflected signal detected by the optical receiver is weak, the maximum measurable range of the laser rangefinder will be reduced as the return signal cannot be detected. For diffuse reflective objects such as buildings and stones, their reflection models can be idealized as shown in Figure 3-6 [73]. The power of reflected light that is perpendicular to the object being irradiated has maximum intensity.

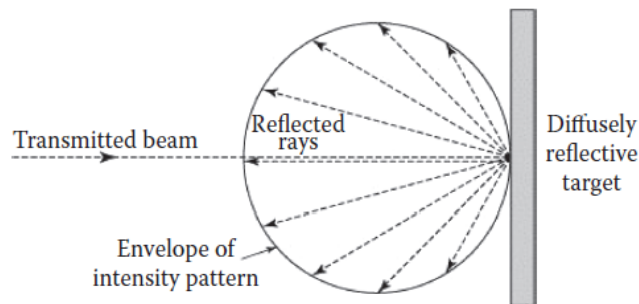


Figure 3-6 The reflection model of diffuse objects [73]

Additionally, the reflectivity of the laser beam varies with its wavelength. Previous research has published tables on laser wavelength and reflectivity based on data provided by laser rangefinder manufacturer RIEGL [75]. The reflectance of a laser with a wavelength of 900 nm to distinct objects is shown in Table 3-1.

Table 3-1 The reflectance of a laser with a wavelength of 900 nm to distinct objects [75]

Material	Reflectivity (%)
Lumber (pine, clean, dry)	94
Snow	80 - 90
White masonry	85

Limestone, clay Up to	75
Deciduous trees Typical	60
Coniferous trees Typical	30
Carbonate sand (dry)	57
Carbonate sand (wet)	41
Beach sand; bare areas in desert Typical	50
Rough wood pallet (clean)	25
Concrete, smooth	24
Asphalt with pebbles	17
Lava	8
Black neoprene (synthetic rubber)	5

3.1.5 Transmission Module

The modulated signal transmitted through the optical system to the atmosphere and reflected from the object is then received by the optical receiving system. The received optical signal pass through the optical signal processing such as collimation, so that the energy can eventually be concentrated in the photodetector for photoelectric conversion. Thus, the transmission module can be summarized as the energy attenuation of the modulated optical signal and the phase delay with respect to the reference signal.

The received echo optical signal can be expressed as [74],

$$P_r = \frac{T^2 \rho D}{2\pi r^2} P_t \quad (3.15)$$

where P_t is the power of the pulse transmitted signal, T is the one-way atmospheric transmission factor, ρ is the reflectivity coefficient of the object, D is the receiving aperture, r is the transmitting distance.

It can be seen from Eq. (3.15) that the laser rangefinder receives only a small fraction of the transmitted pulse power when it propagates to and from the target being measured. As mentioned earlier, before calculating the final phase difference and the measuring distance, it is necessary to amplify the received signal and filter out the noise generated during the propagation.

3.2 Phase Measurement Method

Measuring the phase difference between the two sinusoidal signals with the same frequency is significant in the engineering field. The phase measurement method can be divided into analog and digital methods [76]: the traditional way relies on analog devices, such as diode ring phase detector and pulse counting technology. The measurement system is complex and needs precise devices, high hardware costs. In recent years, the phase measurement method gradually goes to the digital direction. The advantages of the digital method are: low hardware costs, and adaptability. Besides that, the accuracy of the digital method is higher than the analog measurement. Phase measurement is different from the time interval measurement of the pulse method. The phase measurement method has its benefits and disadvantages and the suitable application range. It is critical to choose a set of precise and appropriate phase measurement algorithms for the specific laser rangefinder.

The commonly used methods of digital phase measurement for laser ranging field include digital synchronous detection [77], Fast Fourier Transformation (FFT) method [78] and all phase Fast Fourier Transformation (AP-FFT) method [79].

3.2.1 Digital Synchronous Detection

Synchronous detection technology has been widely used in various applications, especially in the field of telecommunications. The synchronous detection in telecommunication is similar to this phase measurement method, so this method is called "synchronous detection." As can be seen in Figure 3-7, the signal to be analyzed must be mixed with two orthogonal digital reference signals after sampling in digital synchronous detection [62][80].

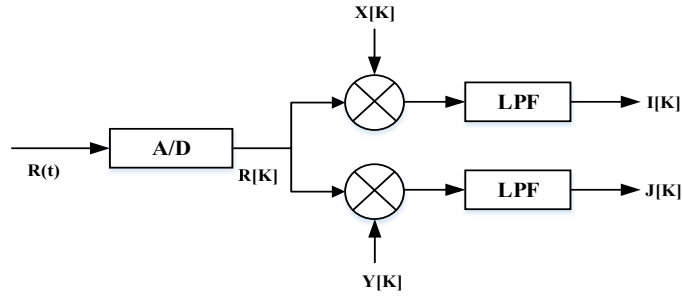


Figure 3-7 The principle of digital synchronous detection

Assuming $R(t)$ is the electrical signal at the receiving part which can be expressed as,

$$R(t) = A \cos(2\pi f_0 t + \theta) \quad (3.16)$$

where A is the amplitude, f_0 is the signal frequency and θ is the phase shift in signal propagation. Through the A/D convertor, the sampled digital signal is.

$$R[K] = A \cos(2\pi f_0 K / F_0 + \theta) \quad (3.17)$$

where F_0 represents the sampling rate. The two orthogonal digital reference signals mixed with the signal $R[K]$ are,

$$X[k] = \sin\left(\frac{2\pi f_0 K}{F_0}\right) \quad (3.18)$$

$$Y[k] = \cos\left(\frac{2\pi f_0 K}{F_0}\right) \quad (3.19)$$

where $X[k]$ and $Y[k]$ have the identical signal frequency f_0 and sampling frequency F_0 . Notice that for a special case when $f_0 = F_0/4$, the two reference signals can be simplified as:

$$X[k] = \sin \frac{K\pi}{2} \quad (3.20)$$

$$Y[k] = \cos \frac{K\pi}{2} \quad (3.21)$$

The values of $X[k]$ and $Y[k]$ can only be 0,1 or -1. Therefore, the following multiplication can be easily achieved. After passing a low pass filter, $I[K]$ and $J[K]$ are shown in Table 3-2.

Table 3-2 Mixing result of the received signal and reference signals

K	I[K]	J[K]
Odd	$\alpha A \sin(\theta)$	0
Even	0	$\alpha A \cos(\theta)$

Therefore, the phase shift θ can be obtain from $I[K]$ and $J[K + 1]$ regardless of the attenuation coefficient α .

Digital synchronous detection using the heterodyne detection technology combined with the synchronous demodulation principle not only has high measurement accuracy but also hold a small amount of data calculation and a fast measurement speed. This method is suitable for high-precision, high-speed phase measurement.

3.2.2 Fast Fourier Transform Method

The Fourier transform can represent any signal satisfying the condition as a sum of many simple sinusoidal signals to derive the spectrum of the signal and to analyze the signal in the frequency domain. In general, if a function satisfies integrable, the Fourier transform can be performed on it [81].

Supposing the original continuous function in the time domain is $x(t)$, the Fourier transform formula of the function can be expressed as:

$$X(\omega) = \int_{-\infty}^{+\infty} x(t)e^{-i\omega t} dt \quad (3.22)$$

Based on the Fourier transform formula, the signal is sampled firstly, and then the FFT operation is performed on the sampled discrete sequence $x(n)$:

$$X(m) = \sum_{n=0}^{N-1} x(n)e^{-j\frac{2\pi}{N}mn} \quad (3.23)$$

where N is the number of sampling points, n is the n^{th} sampling point, m is the number of harmonic, here $m = 1$. Then, the initial phase of the signal can be directly calculated. The real part of $X(m)$ is $Re[X(m)]$, and the imaginary part is $Im[X(m)]$, formulas to obtain the initial phase of two signals and phase difference through $X(m)$ are shown in (3.24), (3.25), (3.26).

$$\varphi_1 = \arctan\left(\frac{Im[X_1(m)]}{Re[X_1(m)]}\right) \quad (3.24)$$

$$\varphi_2 = \arctan\left(\frac{Im[X_2(m)]}{Re[X_2(m)]}\right) \quad (3.25)$$

$$\Delta\varphi = \varphi_1 - \varphi_2 \quad (3.26)$$

For an ideal sine wave signal, the Fourier transform of it contains merely the fundamental harmonic component. However, in the actual measurement, the measured signal is often subject to a variety of noise pollution resulting in reducing the signal-to-noise ratio. When the signal-to-noise ratio maintains at a high standard, the initial phase of the input signal can be gained by calculating the initial phase of the fundamental wave component, and the phase difference of the two input signals can be obtained.

The result of FFT processing of the sinusoidal signal is a sophisticated form with abundant phase information which is a commonly used method in the field of digital phase measurement. However, for the FFT algorithm, to get the precise phase of the signal, it must meet a series of conditions:

1. the sampling frequency must match the Nyquist–Shannon sampling theorem, and sampling is strict integral period sampling;
2. for sampling points, the commonly used radix-2 FFT algorithm requires sampling points must be an integer power of 2.

To meet the above conditions, the stability of signal frequency and sampling frequency are required greatly high. In addition, in the practical application of the signal frequency and sampling frequency, it is impossible to sample the whole cycle of the signal perfectly, there will always be some deviation which causes the spectrum leakage and the signal phase change [82]. So the amplitude and phase error of the signal obtained by directly calculating the FFT will be larger, and the peak error occurs when the signal frequency lies between the two discrete spectral lines. Another flaw is there is a fence effect in the discrete Fourier transform, resulting in a resolution error and the measurement results need to be corrected. At present, the frequency correction methods are iterative frequency estimation method, energy barycenter correction method, ratio method, time-shift phase difference method [83][84][85][86]. For the above methods, the time-shift phase difference method has the highest accuracy of spectral correction.

3.2.3 Ap-FFT Phase Measurement Method

Although the measurement accuracy has improved since FFT has been windowed function processing and spectral correction, the improvement is limited. All-phase FFT (ap-FFT) is a spectral estimation algorithm proposed for solving spectrum leakage of the traditional fast Fourier transform spectrum analysis method. It has the characteristics of the initial phase invariance and the effective prevention of spectrum leakage [79]. Reference [87] mentioned the ap-FFT method has the advantages of accurate phase measurement and no need for synchronous sampling and additional correction measures.

The ap-FFT algorithm can be summarized as follows: the sampled signal to be analyzed is truncated, and $2N - 1$ sample points are taken. These acquired data points are divided into a number of N segments and the length of each segment is N . After the data in each segment are executed periodic extension, the data is aligned according to the position of the N^{th} point data in the original segments. The extended data is truncated by using the length of N rectangular window function. The data in the corresponding location were superimposed to get all-phase pre-processing data. The processed data is subjected to N -point FFT transform, that is the ap-FFT spectrum analysis process. The principle of the ap-FFT method is shown in Figure 3-8.

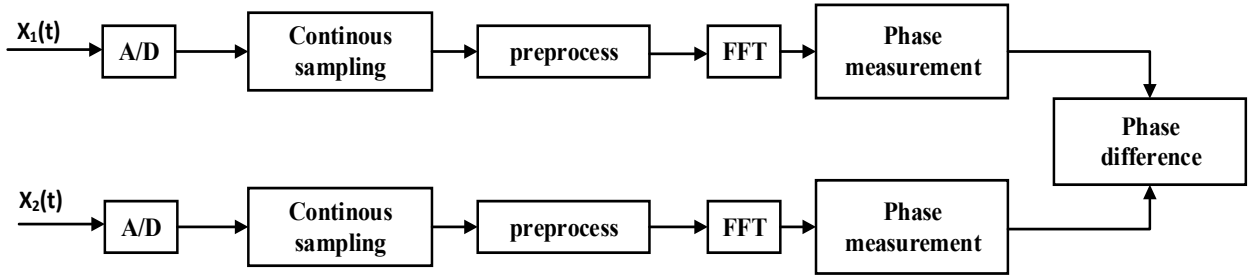


Figure 3-8 The principle of the ap-FFT method

For a point $x(0)$ in the time series, there exists only N N -dimensional vectors containing this point:

$$\begin{aligned}
 x_0 &= [x(0), x(1), \dots, x(N-1)]^T \\
 x_1 &= [x(-1), x(0), \dots, x(N-2)]^T \\
 &\dots \dots \\
 x_{N-1} &= [x(-N+1), x(-N+2), \dots, x(0)]^T
 \end{aligned} \tag{3.27}$$

Each vector is cyclically shifted to move the sample point $x(0)$ to the first position, as shown below.

$$\begin{aligned}
 x_0 &= [x(0), x(1), \dots, x(N-1)]^T \\
 x_1 &= [x(0), x(1), \dots, x(-1)]^T \\
 &\dots \dots \\
 x_{N-1} &= [x(0), x(-N+1), \dots, x(-1)]^T
 \end{aligned} \tag{3.28}$$

These vectors are added together, and the preprocessed data vector can be express as:

$$x_{AP} = \frac{1}{N} [Nx(0), (N-1)x(1) + x(-N+1), \dots, x(N-1) + (N-1)x(-1)]^T. \tag{3.29}$$

All phase spectrum analysis is divided into two steps: data preprocessing and FFT processing. The preprocessing algorithm is shown in Figure 3-9. Preprocessing of the all-phase input data is done by convoluting with a window function and then completes the mapping of the data vector $x = [x(N - 1), \dots, x(0), \dots, x(-N + 1)]^T$ of the length $(2N - 1)$ to the data vector $X_1 = [X_1(0), X_1(1), \dots, X_1(N - 1)]^T$ of length N . According to the different window functions, data preprocessing is divided into three categories: no window, single window and double windows, Hanning double windows preprocessing is generally used [88].

The implementation scheme of the ap-FFT method is shown in Figure 3-9, it can be expressed as:

1. firstly, obtaining the $2N - 1$ sampling points of signal $X(n)$.
2. forming an N -point Hanning window, the Hanning window convolutions itself to obtain a $2N-1$ convolution window $w_1 \times w_2$.
3. summing $2N - 1$ points in this convolution window.
4. each part of the convolution window is divided by the sum of the convolution window to obtain a normalized $2N-1$ points convolution window.
5. the $2N - 1$ points of the input signal are multiplied by the normalized convolution window.
6. the 1st point and $(N + 1)^{th}$ point are added together, 2nd point and $(N + 2)^{th}$ point are added together ... $N-1$ th point and $2N-1$ th point are added together to get the N -point preprocessing sequence.

The second part is implementing the N -point FFT transform for these N points. Then the phase difference is obtained according to the Fourier transform measurement method mentioned above.

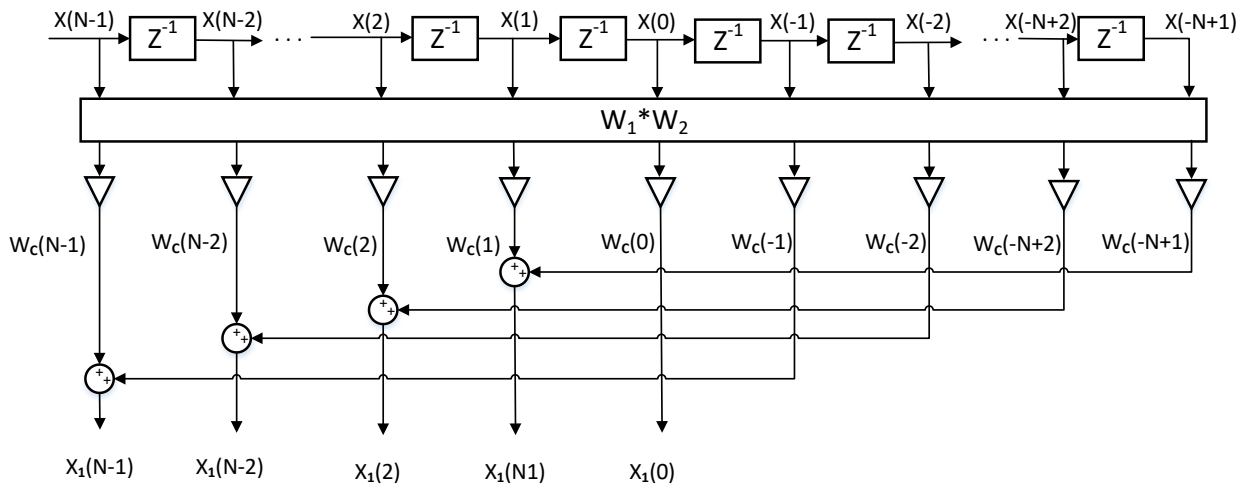


Figure 3-9 The principle of data preprocessing

3.3 Design of Dual-Frequency Pulse Laser Ranging System

The experiment module of the dual-frequency pulse laser ranging system is shown in Figure 3-10. The model comprises a laser modulation transmitting unit, a receiving unit, a signal processing unit and an optical system.

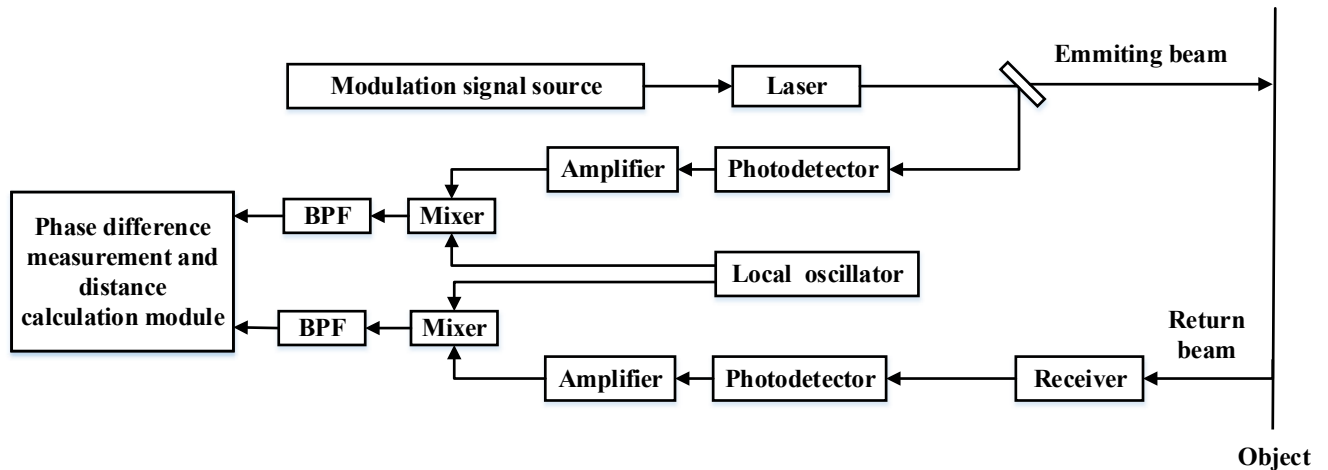


Figure 3-10 Model of dual-frequency pulse laser ranging system

The laser modulation transmitting unit includes a pulse signal source generator and a laser driving circuit. The system adopts a design scheme that transmits two pulse signals. The same-frequency sine signal obtained by processing the low-frequency pulse input signal is used to

roughly calculate the measured target to obtain the approximate value of the measured distance. The sinusoidal signal obtained by signal processing of the high-frequency pulse signal is used to increase the measurement accuracy of the measured distance.

The receiving unit mainly consists of a photoelectric detecting module, the mixing module, and the filtering module. This section receives the echo signals through photoelectric detection, converts the optical signals into photoelectric signals through photoelectric conversion, and then inputs them to the signal processing module through amplification and filtering.

The signal processing module realizes the simultaneous reception of the received signal and the reference signal, completes the corresponding distance calculation and carries on the data fusion to obtain the correct distance measurement result.

The optical system includes the beam emission part, the receiving part, and the inner optical path. The ranging signal is transmitted through the optical path and the electronic circuit by referring to the model mentioned in [89]. After passing the optical path and the electronic circuit, the phase will have a corresponding phase shift. Therefore, the phase of the signal not only contains the phase shift generated from the measured distance but also includes some additional phase shift. The additional phase shift of the electronic circuit changes with the external environment, the performance of the components and its stability [90]. This change is not constant, and there is no law to follow. To eliminate the phase shift through the receiving part, the system adds an inner optical path as the reference path. The beam splitter will divide the laser light into a reference beam and a measuring beam. The measuring optical path and the reference optical path have different receiving circuits which improve the measurement speed and accuracy.

There are two main implementations [91]. For the first method, the selected modulation frequencies are relatively concentrated. The high-frequency signal is used to ensure the accuracy of the system measurement accuracy while adding the lower frequency as an auxiliary frequency. Meanwhile, the two frequencies are very close which will bring the problem of mutual interference. Two decentralized modulation frequencies are used in the other method. Although it will increase the circuit processing bandwidth, the measurement results are more accurate than the first method.

Supposing the returned phase shift of the low-frequency f_l signal is not greater than a sinusoidal period 2π , the distance measured by the low-frequency signal can be expressed as,

$$L_l = \frac{c}{2f_l} \times \frac{\Delta\varphi_l}{2\pi} \quad (3.30)$$

where $\Delta\varphi_l$ is the phase shift of the low-frequency signal. Since the wavelength of the high-frequency generator is much smaller than the measured distance, it can only measure a tiny distance corresponding to a phase shift not greater than a sine wave period.

$$L_h = \frac{c}{2f_h} \times \frac{\Delta\varphi_h}{2\pi} \quad (3.31)$$

where $\Delta\varphi_h$ is the phase shift of the high-frequency signal in one period. The combination of the precision distance data and the coarse measurement distance data gives the total ranging result. Supposing the maximum unambiguous range of the high-frequency signal ranging is $NAR_{f_h} = \frac{c}{2f_h}$, the data convergence algorithm is divided into three steps [77]:

First step: equation (3.30) and (3.31) are used to correct the calculation, resulting in a coarse distance correction value L_{l1} .

$$L_{l1} = L_l + \left(\frac{NAR_{f_h}}{2} - L_h \right) \quad (3.32)$$

Second step: the coarse measurement distance correction value L_{l1} is divided by the maximum unambiguous range of high-frequency component, and then rounding it.

$$L_{l2} = \left\lfloor \frac{L_{l1}}{NAR_{f_h}} \right\rfloor \quad (3.33)$$

Third step: L_h and L_{l2} are merged to get the final distance measurement.

$$L_{final} = L_{l2}NAR_{f_h} + L_h \quad (3.34)$$

3.3.1 Frequency Selection Principle

In the dual-frequency pulse laser ranging method, to ensure the accuracy of ranging with no blurring, two different modulation frequencies are used in the system.

Supposing f_l is the frequency of low-frequency signal and f_h is the frequency of high-frequency signal where $f_h > f_l$. NAR_{f_l} and NAR_{f_h} are corresponding maximum unambiguous ranges where $NAR_{f_l} > NAR_{f_h}$. As the modulation frequency increases, the maximum unambiguous range decreases. When the phase measurement errors are both $\delta\Delta\varphi$, ΔL_l and ΔL_h are the corresponding distance measurement errors where $\Delta L_l > \Delta L_h$. With the increase of the modulation frequency, the accuracy of the distance measurement is gradually improved.

The ambiguity distance obtained by the low frequency f_l is used to solve the maximum unambiguous range problem when the modulation frequency is f_h . The accuracy of the ranging is ΔL_h . So, the method uses low modulation frequency f_l to ensure the unambiguous range, and high modulation frequency f_h to ensure the ranging accuracy.

In the laser ranging system, if the value of f_h / f_l is very small, the measurement system will be complicated. However, due to the limited bandwidth of the ranging circuit, f_h / f_l cannot be infinitely increased. According to the dual-frequency ranging process, the unambiguous distance NAR_{f_h} of the modulation frequency f_h (the measurable distance corresponding to the modulation frequency f_h) should be greater than the distance measurement accuracy ΔL_l obtained by the low-frequency signal which can be expressed as [77],

$$NAR_{f_h} > \Delta L_l \quad (3.35)$$

where ΔL_l can be calculated by:

$$\Delta L_l = \frac{c}{2f_l} \times \frac{\delta\Delta\varphi}{2\pi} \quad (3.36)$$

Equation (3.35) can be reduced to:

$$\frac{f_h}{f_l} < \frac{2\pi}{\delta\Delta\varphi} \quad (3.37)$$

Equation (3.37) is the principle of frequency selection. The low modulation frequency is selected according to the measurement range; the selection of the high modulation frequency is based on the measurement accuracy requirements.

On the occasion that the modulation frequencies are 15 MHz and 150 KHz, the phase measurement error is 0.36° , the maximum unambiguous range and ranging resolution corresponding to the two frequencies are shown in Table 3-3. Correspondingly, the frequencies of the local oscillator are selected as 14.99 MHz and 140 KHz. In such a manner, after the mixed signal passes through a low-pass filter, a low-frequency signal of 10 KHz can be obtained.

Table 3-3 Maximum unambiguous range and ranging resolution of two frequencies

Frequency	Maximum unambiguous range	Ranging resolution
15 MHz	10m	10 mm
150 KHz	1000m	1000 mm

When the modulation frequency increases, it not only improves the accuracy of the phase measurement and ranging precision but also expands the system's bandwidth that will introduce noise and reduce the signal to noise ratio. In some applications, it is necessary to consider all aspects of the factors in the system to achieve the best performance.

3.4 Design of Signal-Frequency Pulse Laser Ranging System

The ranging module of the signal-frequency pulse laser system is shown in Figure 3-11.

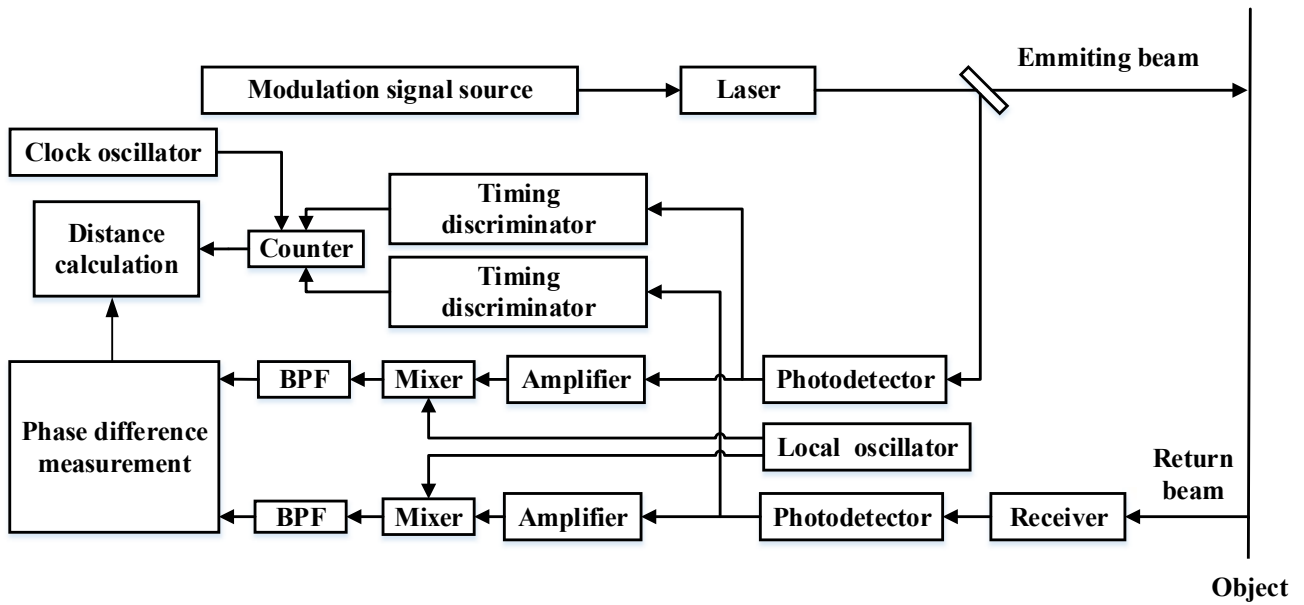


Figure 3-11 Model of signal-frequency pulse laser ranging system

Different from the dual-frequency method, signal-frequency pulse laser system uses only a single-frequency signal as the measurement signal. At the receiving end, the echo signal is divided into two paths. The pulse measurement part completes the rough measurement, and the phase shift measurement part is used to improve the measurement precision.

The pulse interval calculation section consists of a time discrimination unit and a time interval measurement unit. The signals obtained after judging the timing of the start time and the end time by the constant fraction method are transmitted to the time interval measuring unit. Since the pulse measurement part is only responsible for the rough measurement of the distance and does not need to obtain extremely high accuracy, the time interval measurement module adopts the direct counter method, which is advantageous for reducing the design difficulty and circuit complexity. The counter passes the number of pulses transmitted by the clock oscillator to the distance calculation unit to accomplish rough measure.

Supposing N_c is the output number of the counter, f_{co} is the frequency of the clock oscillator, the distance measured by time interval can be expressed as,

$$L_s = \frac{N_c}{f_{co}} \times C/2 \quad (3.38)$$

where C is the speed of light. For the phase calculation part, the distance obtained from phase difference can be expressed as.

$$L_p = \frac{c}{2f} \times \frac{\Delta\varphi}{2\pi} \quad (3.39)$$

where f is the frequency of pulse signal, $\Delta\varphi$ is the phase difference of sinusoidal signals in one period.

Similar to the dual-frequency pulse ranging method, in the distance calculation module, the combination of the pulse measuring result and the phase difference measuring result is also divided into three parts.

First step: from equation (3.38) and (3.39), the coarse distance correction value L_s can be expressed as,

$$L_{l1} = L_s + \left(\frac{NAR_f}{2} - L_p \right) \quad (3.40)$$

where NAR_f is the non-ambiguity range of the sinusoidal signal with the frequency of f .

Second step: the coarse measurement distance correction value L_{l1} is divided by NAR_f , and then taking the integer part.

$$L_{l2} = \left\lfloor \frac{L_{l1}}{NAR_f} \right\rfloor \quad (3.41)$$

Third step: L_p and L_{l2} are merged to get the final distance measurement.

$$L_{final} = L_{l2}NAR_f + L_p \quad (3.42)$$

3.4.1 Frequency Selection Principle

For the signal-frequency pulse laser system, equation (3.35) can be rewritten as,

$$NAR_f > \Delta L_{co} \quad (3.43)$$

where NAR_f is the maximum non-ambiguity range of the phase measurement part and ΔL_{co} is the distance measurement error of time interval measurement part. Assuming the frequency of clock oscillator is 150 MHz, ΔL_{co} could reach to:

$$\Delta L_{co} = \frac{c}{2 \times f_{co}} = \frac{3 \times 10^8}{2 \times 150 \times 10^6} = 1m \quad (3.44)$$

Eq. (3.43) can still be tenable when the transmitting frequency is 15 MHz as NAR_f is 10m.

3.5 Error Analysis of Measurement System

3.5.1 Light Velocity Error

The light speed value in the vacuum is an essential theoretical basis in the hybrid pulse and phase-shift laser ranging system, the vacuum speed measurement error will undoubtedly bring the deviation into the distance measurement result. After the 17th century, the national physicists continued to take various means to measure the speed of light, and the precision was continually improved. The value of the speed of light in vacuo is $c_0 = 299792458 \pm 1.2 \text{ m/s}$, which is the international common value. The corresponding distance error effect is expressed as

$$\frac{\Delta c_0}{c_0} = 4 \times 10^{-9} \quad (3.45)$$

Supposing the measured distance $L = 100m$, the maximum distance error caused by the measurement of the speed of light is $\Delta L_f = 4 \times 10^{-7}m$. The accuracy is precise enough, so the influence of light velocity c_0 on the distance measurement error is insignificant. Therefore, the influence of it can be ignored.

3.5.2 Influence of Modulation Frequency

The function of ranging distance measured by the phase difference is shown below,

$$L = \frac{\lambda}{2} \times \frac{\Delta\varphi}{2\pi} = \frac{c}{4\pi} \times \frac{\Delta\varphi}{f} \quad (3.46)$$

where c is the speed of light propagation in vacuum, f is the signal frequency and $\Delta\varphi$ is the phase difference between the transmitted signal and the echo model.

According to equation (3.46), if the actual modulation frequency of the oscillation is not equal to the expected frequency that will cause the ranging error which is called the frequency error. The equation is given in (3.47).

$$\Delta L = \frac{c}{4\pi} \times \frac{\Delta\varphi}{f} = \frac{c}{4\pi} \times \frac{\Delta\varphi}{f + \Delta f} \quad (3.47)$$

For a case where the final ranging accuracy is 0.5 mm and the frequency after signal processing is 10 kHz, the measurement range of the phase difference is $[0, 2\pi]$. According to Eq. (3.47), the maximum frequency deviation Δf should be in the range of $3 \times 10^{-4} \text{ Hz}$.

Table 3-4 Crystal oscillator product data

Model	Manufacturers	Working frequency	Frequency stability	Phase noise	Annual aging rate
CO-714	Vectron	32 KHz~25 MHz	$2 \times 10^{-8} \text{ Hz}$	-150 dB	$3 \times 10^{-7} / \text{year}$
CO-750	Vectron	5 MHz ~25 MHz	$5 \times 10^{-8} \text{ Hz}$	-150 dB	$2 \times 10^{-6} / \text{year}$
MV103	Morion	10 MHz~40 MHz	$7.5 \times 10^{-9} \text{ Hz}$	-155 dB	$3 \times 10^{-8} / \text{year}$
MV118	Morion	10 MHz~25 MHz	$1 \times 10^{-8} \text{ Hz}$	-150 dB	$3 \times 10^{-8} / \text{year}$

As can be seen from Table 3-4, the accuracy of the frequency stability of most crystal oscillators can meet the requirements.

3.5.3 Phase Measurement Error

The factors that cause the phase measurement error are the wrong phase measurement principle, the meteorological condition, the signal crosstalk between the received signal and the transmitted signal [92].

The error of the phase measurement principle is caused by the inaccuracy of the phase measuring device and measured signal during transmitting. When the photoelectric conversion of the receiving device is carried out, the photoelectric conversion time depends on the sensitivity of the photosensitive surface of the instrument and the time of photoelectron crossing. Due to the different performance of the photosensitive material, the variation in the manufacturing of the receiving device will cause the phase nonuniformity of the receiving device. The influence of meteorological conditions is mainly caused by the ambient light, atmospheric turbulence, atmospheric attenuation and absorption, and the sunlight. Signal crosstalk between the received signal and the transmitted signal also causes additional phase errors. The ranging measurement error generated by the phase error is related to the modulation frequency, and the influence of the phase error on the ranging error is shown in Figure 3-12.

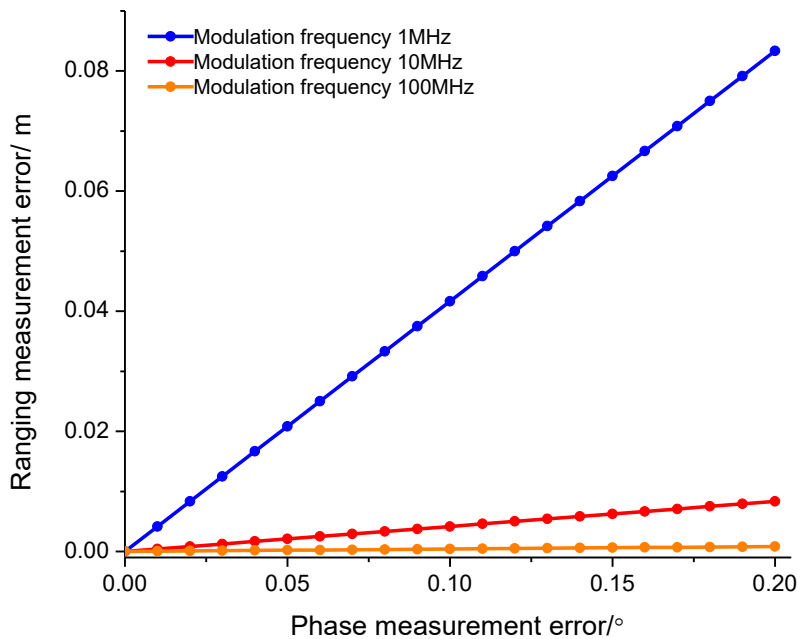


Figure 3-12 The effect of phase measurement error on distance measurement error

As can be seen from Figure 3-12, for a fixed phase measurement error, the higher the modulation frequency is, the smaller the measurement error is. For the equivalent phase measurement error, the modulation frequency can be increased to ensure high measurement accuracy. However, increasing the modulation frequency will reduce the corresponding maximum unambiguous range. For a high-frequency signal, it is hard to ensure the excellent accuracy of the

phase measurement. Also, the choice of high modulation frequency improves not only the demand of the laser modulation drive system but also the corresponding receiving system bandwidth is not conducive to the subsequent circuit system design and implementation. Increasing the bandwidth of the receiving system will enlarge the circuit noise and interference and reduce the signal-to-noise ratio. In the choice of the modulation frequency, these several factors need to be taken into consideration.

Chapter 4 Simulation of Phase-Detection Performance and Laser Ranging System

In the hybrid pulse and phase-shift laser ranging system, the correctness of the phase measurement is the most critical factor in assuring the accurate ranging. This chapter will focus on the phase measurement ability of three commonly used phase measurement methods in the phase-shift laser ranging system. In the background of frequency offset, white Gaussian noise and harmonic, the accuracy of phase discrimination is simulated by MATLAB software. Finally, the transmitting unit, the receiving unit and the signal processing unit of two proposed ranging models are created in Optisystem-MATLAB co-simulation package. The simulation results are analyzed to verify the feasibility and correctness of two proposed structures. The simulation experiments provide a theoretical basis for the realization of high-precision hybrid pulse and phase-shift laser ranging systems.

4.1 Simulation of Phase-Detection Performance

The spectral characteristics of the digital synchronous detection method, FFT method and ap-FFT method were simulated by MATLAB software to determine the selected phase-detection method. Since both remaining frequencies of two proposed methods are 10 KHz after the received signal and local oscillator signal doing the difference frequency calculation, the simulated frequency is $f = 10 \text{ KHz}$, the number of sampling points is 512. For simplicity, the following sections and figures use DSD to represent the digital synchronous detection method.

4.1.1 The effect of Frequency Offset

In an actual ranging system, it is difficult for the signal source to produce a completely stable, single frequency component. The frequency stability and spectral purity will directly affect the accuracy of the phase detection. Under the influence of frequency offset, the phase error is related to the phase difference of the signals. The initial phase of the transmitted signal is set to zero, and the phase of the received signal changes between $[0, 2\pi)$. Under distinct phase differences, the phase discrimination deviation is shown in Figure 4-1 and Figure 4-2.

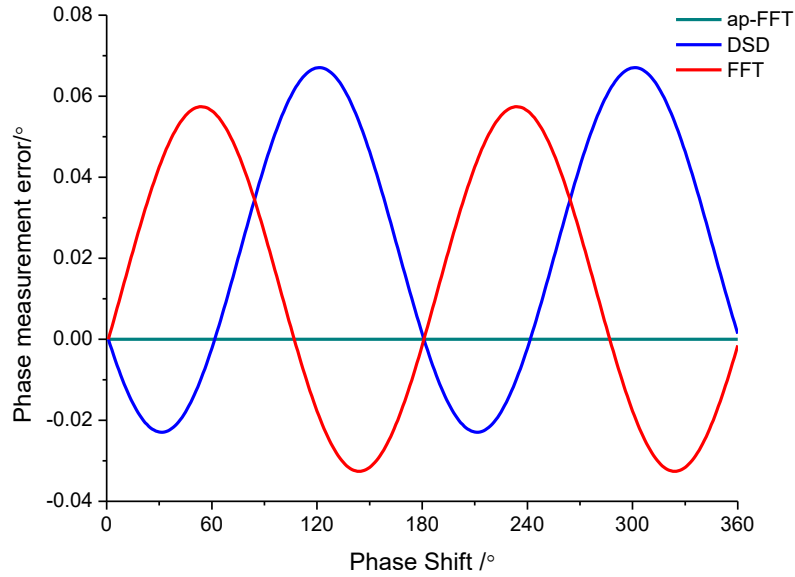


Figure 4-1 Error of measurement with different phase shift at 9.99 KHz

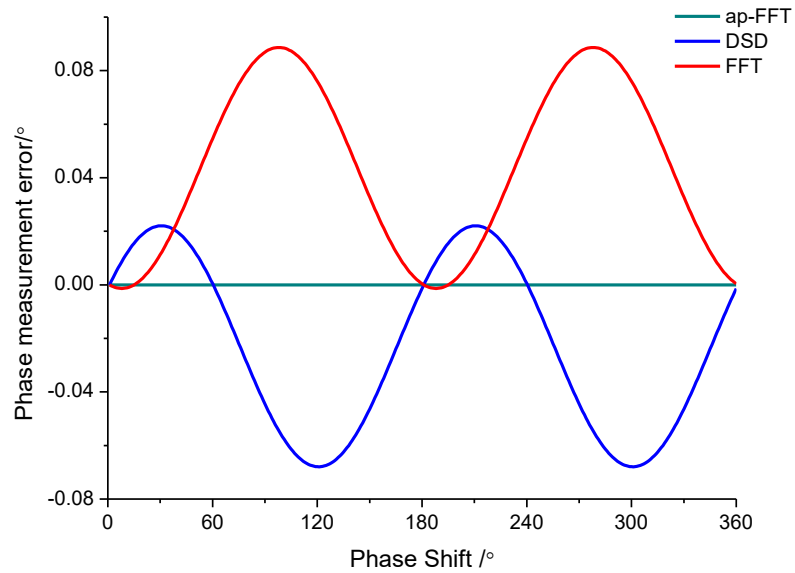


Figure 4-2 Error of measurement with different phase shift at 10.01 KHz

From Figure 4-1 and Figure 4-2, it can be seen that the phase error of the DSD method and FFT method exhibit phase differences with sinusoidal fluctuations when the frequency offset is ± 10 Hz. The performance of the two methods differs depending on the frequency offset. However, for ap-FFT method, it has excellent resistance to the frequency offset.

The normalized frequency offset is set to $\delta \in [-0.0005, 0.0005]$. The actual sinusoidal signal frequency can be expressed as,

$$f_a = f(1 + \delta) \quad (4.1)$$

where the sampling frequency $f_s = 40 \text{ KHz}$, the number of sampling points is 512. The experimental signals used in the simulation are shown as:

$$S_1(n) = \cos\left(\frac{2\pi n}{f_s} \times f_a + \frac{\pi}{3}\right) \quad (4.2)$$

$$S_2(n) = \cos\left(\frac{2\pi n}{f_s} \times f_a + \frac{\pi}{6}\right) \quad (4.3)$$

where the phase difference between the two signals is 30° , and the relationship between the phase measurement error and the frequency offset is shown in Figure 4-3.

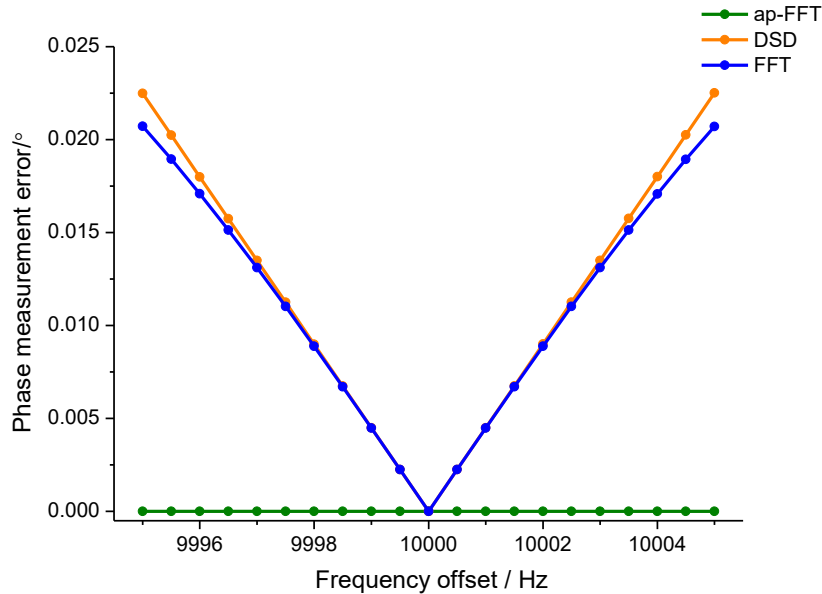


Figure 4-3 Comparison of phase error under frequency offset

It can be seen from Figure 4-3 that the frequency offset causes the phase measurement error in DSD and FFT method. The further away from the center frequency, the larger the error. Ap-FFT method can suppress the influence of the frequency offset well. The error from ap-FFT method is tiny and the measurement result is almost close to the actual value. With a fixed phase

difference, ap-FFT method is more resistant to the frequency offset. Accordingly, the performance of the ap-FFT method is better than DSD and FFT method when the signal has a frequency offset.

4.1.2 The Effect of White Gaussian Noise

To calculate the influence of white Gaussian noise on the phase measurement accuracy of DSD method, FFT method and ap-FFT method, the simulated test signals are,

$$S_1(n) = \cos\left(\frac{2\pi n}{f_s} \times f + \frac{\pi}{3}\right) + x(n) \quad (4.4)$$

$$S_2(n) = \cos\left(\frac{2\pi n}{f_s} \times f + \frac{\pi}{6}\right) + x(n) \quad (4.5)$$

where $x(n)$ is random white Gaussian noise, signal frequency $f = 10\text{KHz}$, sampling frequency $f_s = 40\text{KHz}$, the number of sampling points is 512 and the phase difference between the two signals is 30° . The signal-to-noise ratio of the measured signal is set between 25 dB ~ 55 dB. SNR is reflected by the amplitude ratio of the noise signal and the measured signal. After executing 1000 simulations at different SNRs, the mean values and errors of phase difference measurement under white Gaussian noise are shown in Figure 4-4 and Figure 4-5, respectively.

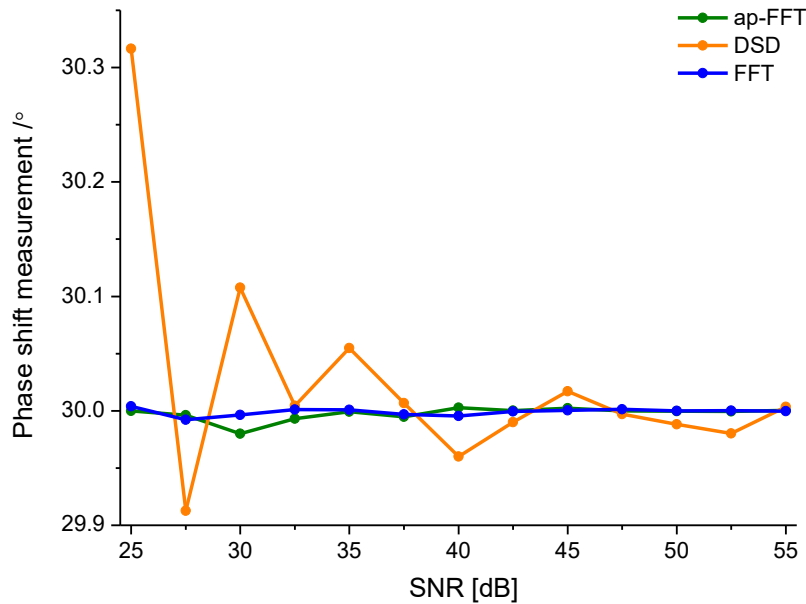


Figure 4-4 Mean value of phase shift measurement under white Gaussian noise

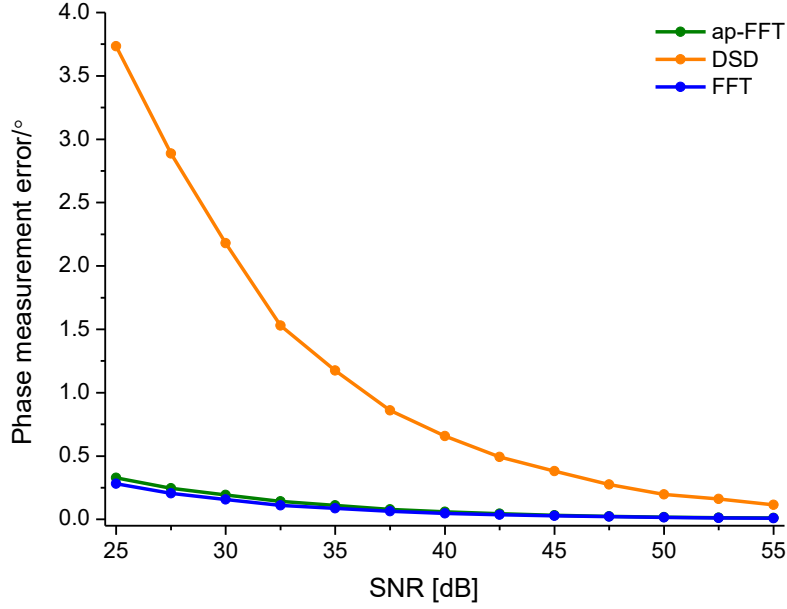


Figure 4-5 Comparison of phase error under white Gaussian noise

As can be seen from Figure 4-4 and Figure 4-5, the precision of the three methods is reduced with the decrease of the signal-to-noise ratio. For DSD method, the mean of the measured phase difference deviates significantly from actual values as the signal-to-noise ratio decreases. When the signal-to-noise ratio is greater than 40 dB, both FFT and ap-FFT have high inhibition of white Gaussian noise, the phase errors of two results are almost the same. When the signal-to-noise ratio is lower than 35 dB, the precision of FFT method is slightly higher than ap-FFT method.

4.1.3 The Effect of Harmonic

Considering the effect of harmonic interference on the phase discrimination performance, different harmonic components are added to the simulated signals. Two signals containing harmonics can be represented as,

$$S_1(n) = \cos\left(\frac{2\pi n}{f_s} \times f + \frac{\pi}{3}\right) + \frac{1}{100} \cos\left(\frac{2\pi n}{f_s} \times f \times Hm + \frac{\pi}{3}\right) \quad (4.6)$$

$$S_2(n) = \cos\left(\frac{2\pi n}{f_s} \times f + \frac{\pi}{6}\right) + \frac{1}{100} \cos\left(\frac{2\pi n}{f_s} \times f \times Hm + \frac{\pi}{6}\right) \quad (4.7)$$

where $Hm = 2, 3, \dots, 8$. Assuming the harmonic signal's power is $\frac{1}{100}$ of the emitted signal power.

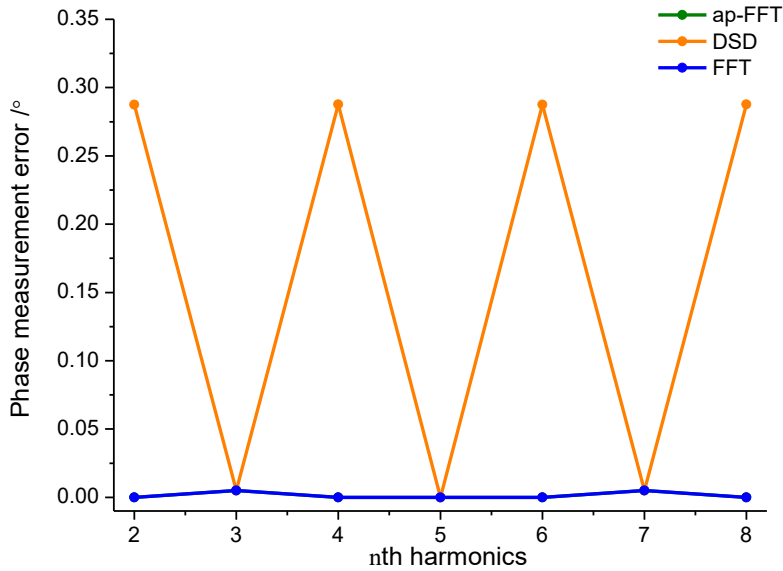


Figure 4-6 Comparison of phase error with harmonics

Figure 4-6 shows that under different harmonic disturbances, the phase errors of FFT and ap-FFT method are less than or equal to DSD method. Therefore, FFT and ap-FFT method are more resistant to harmonic interference.

4.1.4 The Effect of Frequency Offset, White Gaussian Noise and Harmonics

From the above analysis, it is shown that FFT method and ap-FFT method are more accurate than the digital synchronous detection method in each case with the same sampling frequency. For selecting a phase difference detection method applicable to the proposed measurement systems, the effects of frequency offset, white Gaussian noise and harmonics coexist simultaneously in the actual situation, the phase discrimination capabilities of three methods will be analyzed.

The normalized frequency shift of the measured signal is set to $\delta = 0.0001$ with second harmonic, and the SNR changes every 2.5 dB in the range of 25 dB ~ 55 dB. The phase measurement error under the influence of three factors is shown in Figure 4-7 and Figure 4-8.

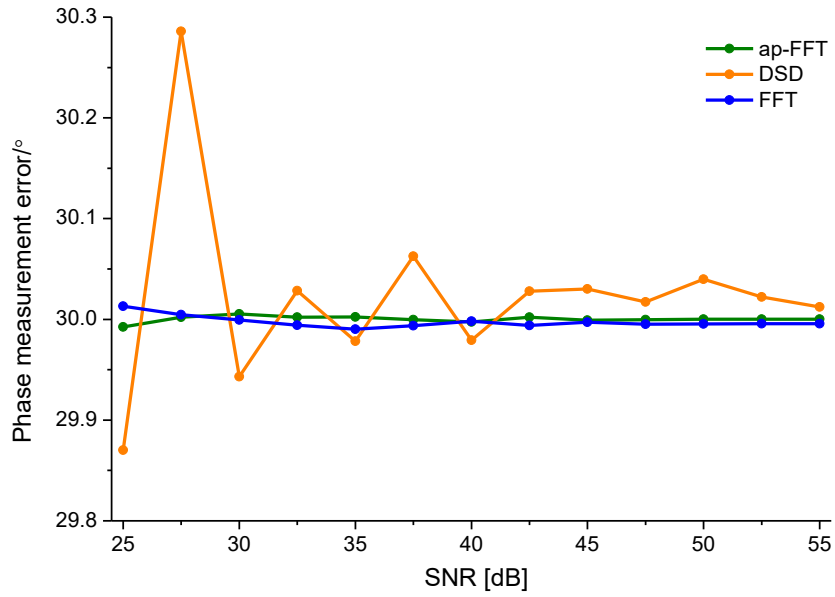


Figure 4-7 Mean value of phase shift measurement

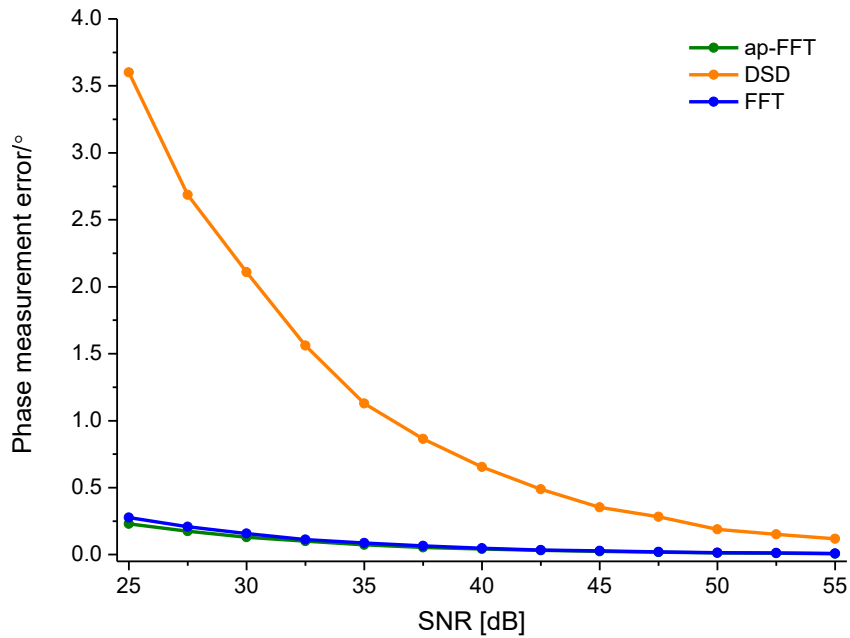


Figure 4-8 Comparison of phase error under frequency offset, white Gaussian noise and harmonics

As can be seen from Figure 4-7 and Figure 4-8, with the increase of SNR, the phase detection performance of the three methods is gradually improved. When SNR is greater than 40 dB, FFT method has a phase-detection accuracy of about 0.048° , the ap-FFT method has a phase-detection accuracy of about 0.041° , and the digital synchronous detection method has a phase-

detection accuracy of about 0.655° . Therefore, when the modulation frequency is 15 MHz, the ranging accuracy of FFT method is 1.3 mm, the ranging accuracy of the ap-FFT method is 1.1 mm, while the ranging error of the digital synchronous detection method is greater than 18 mm. As the SNR decreases, the performance differences increase significantly, and the error curve of the ap-FFT method is always at the bottom.

Consequently, the ap-FFT phase detection method can still maintain superior performance under the influence of numerous factors and realizes high-accuracy phase difference measurement, which can be adopted in the combination of pulsed and phase laser ranging systems.

4.1.5 The Influence of Sampling Points on Phase Accuracy

The above analysis shows that the ap-FFT method can achieve higher accuracy than other mentioned methods when the number of sampling points is 512. In this section, the phase measurement accuracy of the sampling points of 512 points, 1024 points and 2048 points and 4096 points are analyzed.

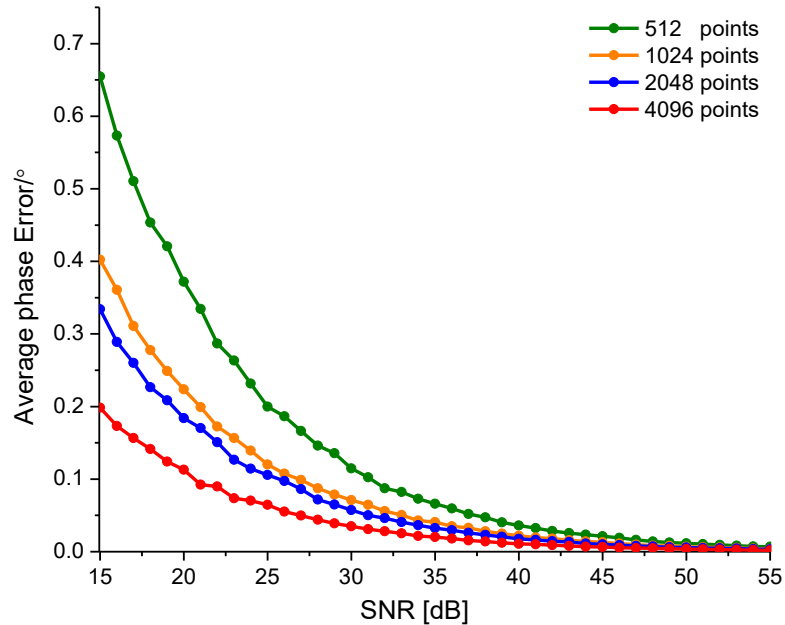


Figure 4-9 Comparison of phase error with different sampling points

As can be seen from Figure 4-9, the phase measurement error decreases as the number of sampling points increases. When the SNR is 20 dB, the average phase error of 4096 sampling

points can achieve 0.1 degrees, and the corresponding ranging error can reach 2.8 mm. While the average phase error of 512 sampling points is 0.35 degree and the corresponding ranging error is 9.7 mm. However, the number of sampling points cannot be infinitely increased which will increase the signal processing time. Hence, the need for precision according to the system requires a reasonable choice of sampling points.

4.2 Simulation of Laser Ranging System

The proposed dual-frequency and signal-frequency pulse laser ranging systems are modeled by using Optisystem and MATLAB co-simulation. OptiSystem is a simulation software for optical links and signal processing circuits. Optisystem is used to generate the modulation signal, establish laser transmitting and receiving models, and build up signal processing procedure. There is an interface that can be used for data transmission with MATLAB in Optisystem. The channel and target model, phase difference calculation, pulse counting process, and final distance measurement are simulated in MATLAB.

The main parameters utilized in two simulation models are shown in Table 4-1. The parameters of the laser source and APD simulated in Optisystem are determined by the datasheet of produced semiconductor laser and avalanche photodiode. The proposed simulation models are tested in different ranging distance and sampling points. The developed models are simulated to display the application and the performance of each proposed system. Eventually, ranging results from two simulation models are compared with the previous works.

Table 4-1 Main simulation parameters

Parameter	Simulated value
Laser source	Center wavelength: 905 nm Peak power: 30 W Slope efficiency: 0.75 W/A Threshold current: 0.75 A Pulse width: 8 ns
Channel and target model	Atmospheric loss factor: 0.8 Target reflectivity: 0.7 Receiver aperture diameter: 15 cm

Photodetector	Peak sensitivity wavelength: 905nm Gain: 100 Responsivity@905nm: 60 A/W Dark noise: 0.05 nA Thermal power density: 0.1 pA/Hz ^{.5}
Bandpass filter	Center frequency: 10 KHz Bandwidth: 2KHz Insertion loss: 0.3 dB
A/D converter	Sample rate: 10 MHz

4.2.1 Dual-Frequency Hybrid Pulse and Phase-Shift Laser Ranging Model

The structure of dual-frequency hybrid pulse and phase-shift laser ranging model using Optisystem is shown in Figure 4-10. Free space channel model is created in MATLAB by using the mathematical configuration. The MATLAB component is created to deliver sampled signals from A/D converter to MATLAB. The phase difference calculation by using ap-FFT and distance computation is executed in MATLAB.

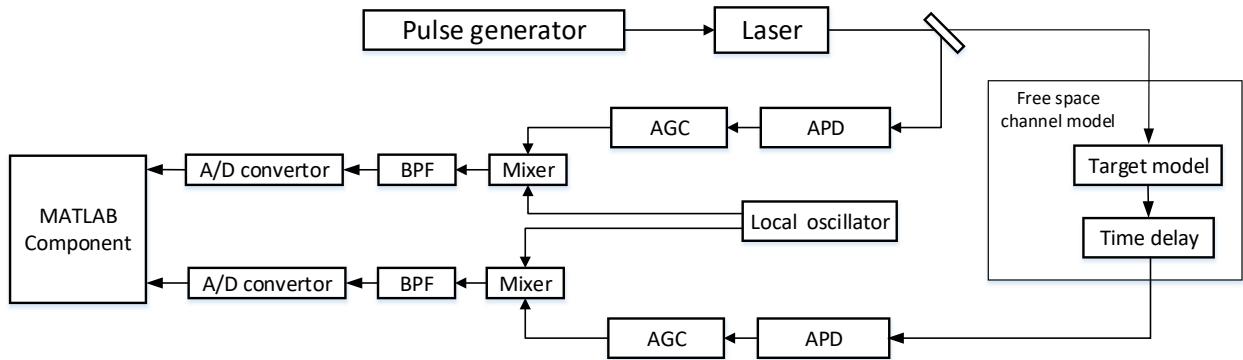


Figure 4-10 Simulated dual-frequency hybrid pulse and phase-shift laser ranging system

In the simulation, 15 Mhz and 150 KHz pulse modulation signals are selected. At the receiving part, 14.99 Mhz and 140 kHz sinusoidal signals are adopted to generate a low-frequency signal with 10 KHz. When setting the ranging distance to 100 m, Figure 4-11 and Figure 4-12 show the reference signal and measured signal obtained after band-pass filtering.

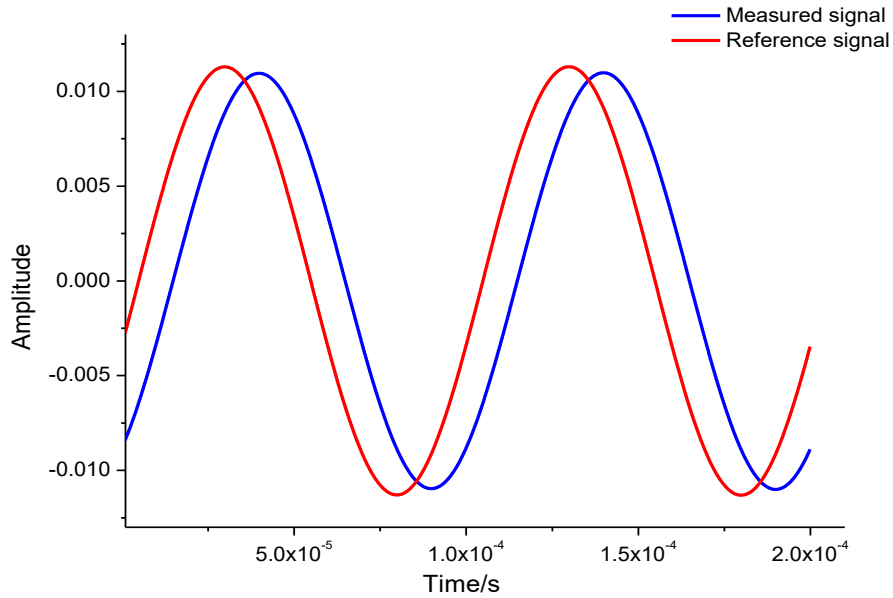


Figure 4-11 Waveforms of the reference and measurement signal when the signal frequency is 150 KHz

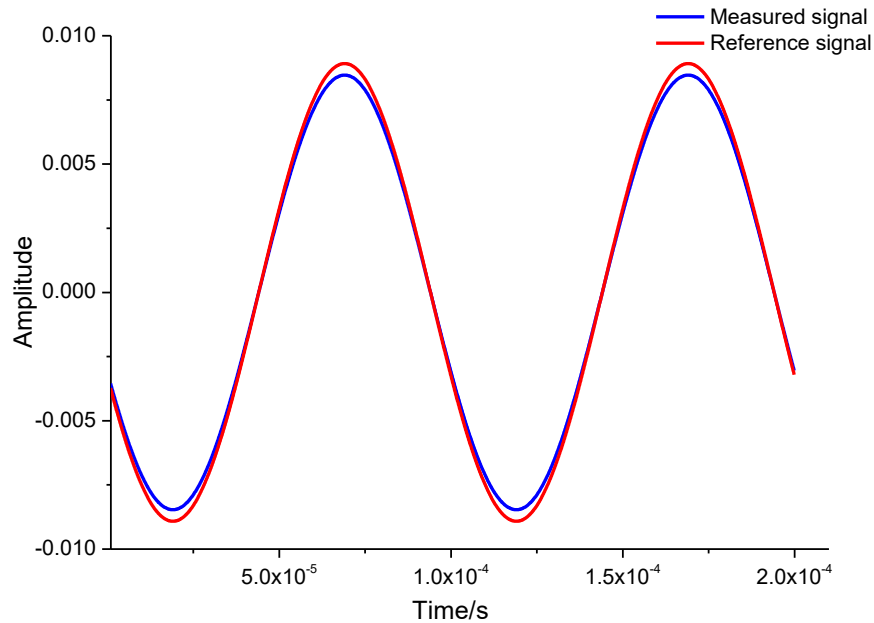


Figure 4-12 Waveforms of the reference and measurement signal when the signal frequency is 15 MHz

It can be seen from two figures that after the photoelectric conversion, amplification, mixing and bandpass filtering, stable reference signals and measurement signals of two modulation frequencies including the phase difference related to the measured distance are obtained, which is the foundation of high precision laser ranging.

The phase difference is calculated by ap-FFT method, and the number of the sampling is 2048. After 200 simulations, the phase difference measurement results are shown in Figure 4-13 and Figure 4-14. The corresponding ranging distance result by merging the above two outcomes is shown in Figure 4-15.

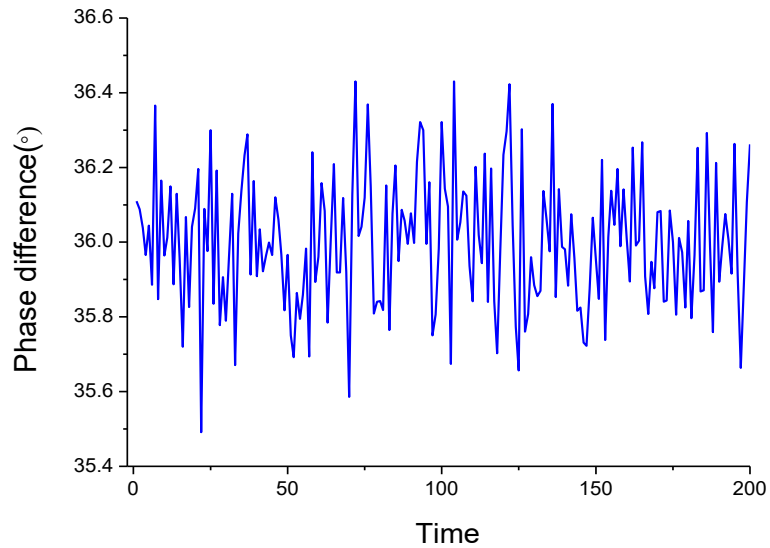


Figure 4-13 Phase difference between the reference signal and measured signal when the signal frequency is 150 KHz

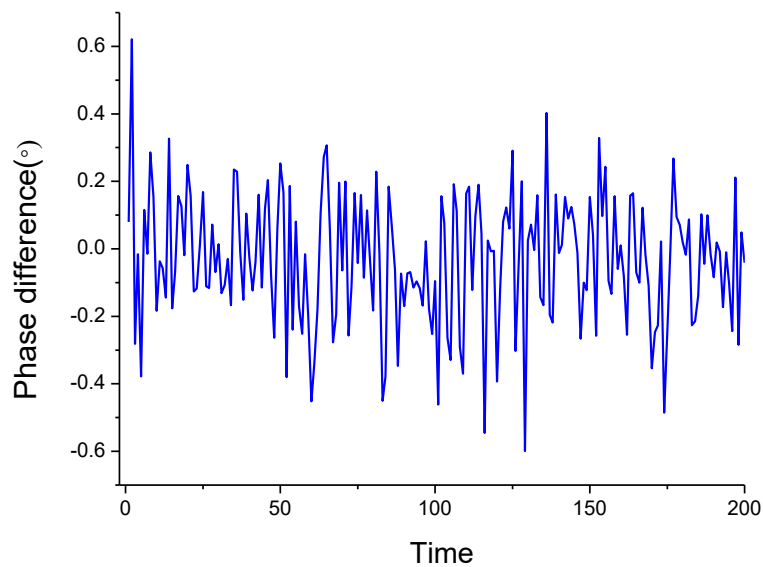


Figure 4-14 Phase difference between the reference signal and measured signal when the signal frequency is 15 MHz

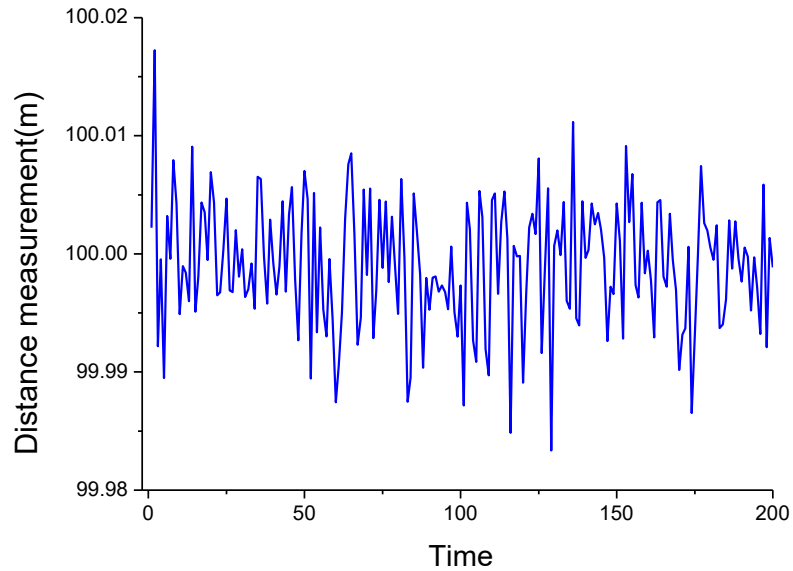


Figure 4-15 Distance measurement result when the ranging distance is 100m

As can be seen from Figure 4-15, when the ranging distance is 100 m, the maximum ranging error is 1.69 cm, the standard deviation of the ranging result is 0.48 cm.

Furthermore, the ranging distance is set to 20.6 m, 50 m, 500 m, 963.15 m, and the number of sampling points is set to 512,1024 and 2048. The standard deviation and the worst case of distance measurement are shown in Table 4-2.

Table 4-2 Simulation results of the dual-frequency hybrid pulse and phase-shift laser ranging model

		Distance measurement error(cm)					
		Standard deviation			Worst case		
Distance(m)	Sampling points	512	1024	2048	512	1024	2048
20.6		0.25	0.25	0.23	0.76	0.65	0.52
50		0.36	0.35	0.32	1.33	1.25	0.93
100		0.60	0.56	0.48	2.05	1.88	1.69
500		2.32	2.21	2.15	6.50	6.35	5.70
963.15		3.97	3.72	3.40	15.7	13.6	12.0

As can be seen from Table 4-2, the ranging accuracy of dual-frequency hybrid pulse and phase-shift laser ranging model decreases as the ranging distance increases. More sampling points always get better-ranging precision. When using the number of sampling points is 2048, the maximum distance error is less than 12 cm, and the ranging standard deviation is less than 3.5 cm. The simulation result can prove the designed dual-frequency hybrid pulse and phase-shift laser ranging system has achieved high ranging accuracy.

4.2.2 Single-Frequency Hybrid Pulse and Phase-Shift Laser Ranging Model

The single-frequency hybrid pulse and phase-shift laser ranging model is simulated by Optisystem as shown in Figure 4-16. In the simulation, 15 MHz pulse modulation signal and 14.99 MHz local reference signal are used to get a 10 KHz low-frequency signal. The MATLAB component sends sampled sinusoidal signals from A/D converter and pulse signals to MATLAB simultaneously.

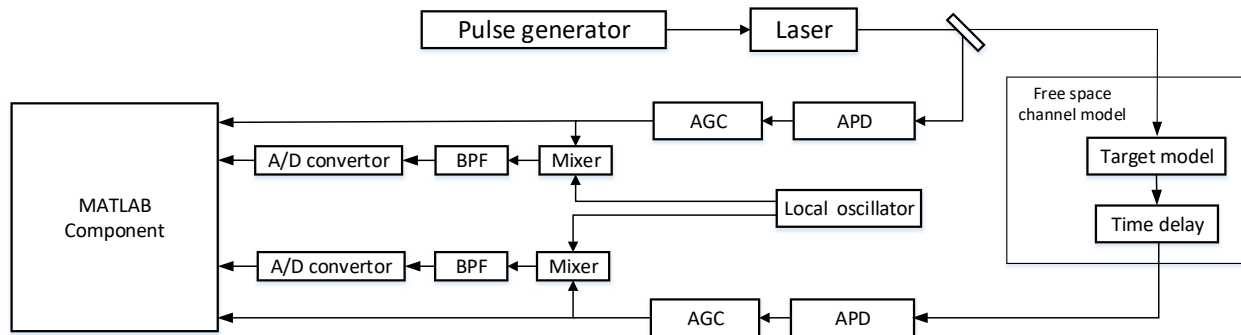


Figure 4-16 Simulated single-frequency hybrid pulse and phase-shift laser ranging system

For the phase-shift part, the phase difference is calculated by the ap-FFT method. The pulse counting part is operated in Simulink as shown in Figure 4-17. After passing through the constant fraction discriminator, received signal and the reference signal are used to start and stop the counter from recording the number of pulses from a local oscillator.

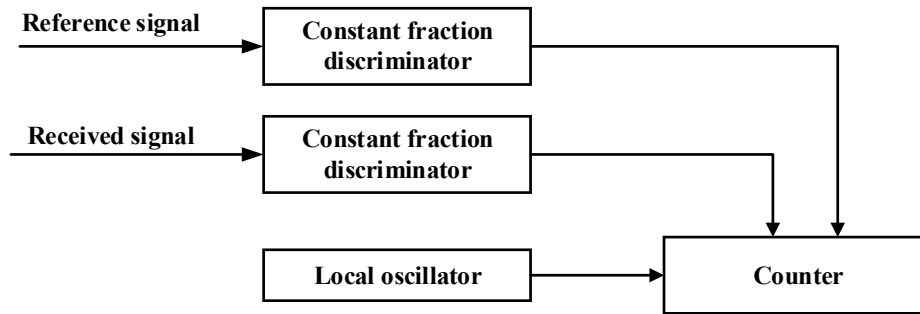


Figure 4-17 Pulse counting part in Simulink

When setting the ranging distance to 100 m, Figure 4-18 shows the reference signal and measured signal obtained after filtering.

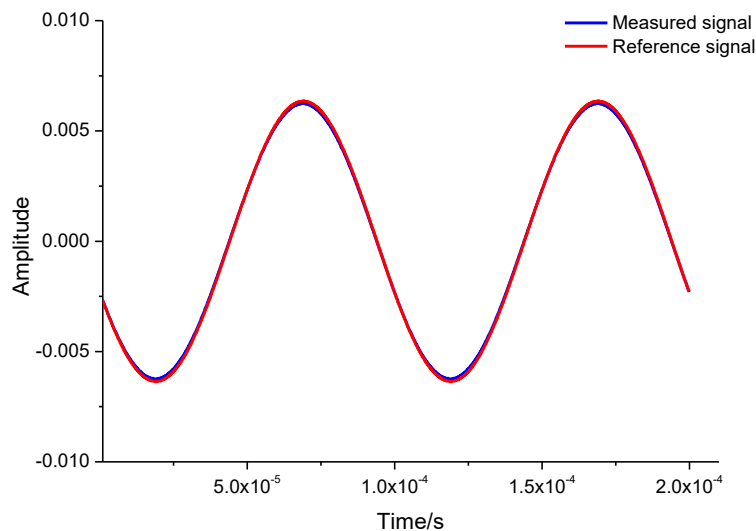


Figure 4-18 Phase difference between the reference signal and measured signal when the signal frequency is 15 MHz

As can be seen from Figure 4-18, since it is an integer multiple of the wavelength when the transmission distance is 100 meters, the phase difference between the measured signal and the reference signal should theoretically be 0° . The phase difference is calculated by the ap-FFT method, and the number of the sampling is 2048. After 200 simulations, the phase difference measurement results are shown in Figure 4-19. The corresponding ranging distance result by merging the phase difference and the pulse counting result is shown in Figure 4-20.

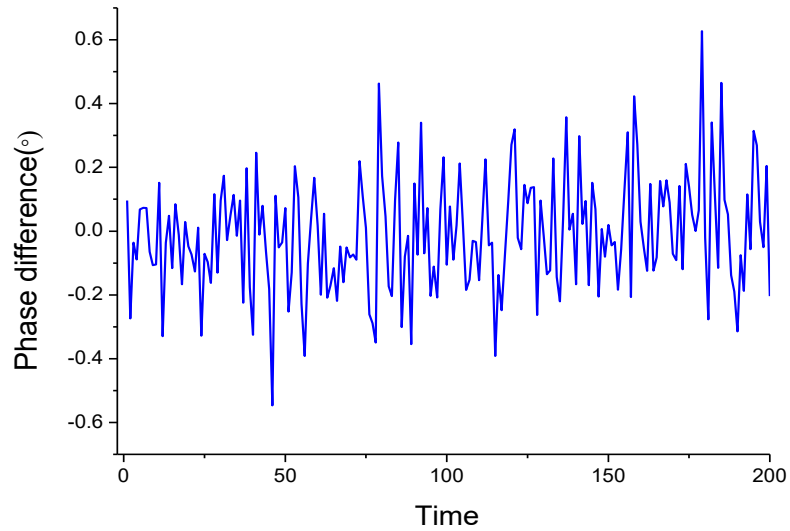


Figure 4-19 Phase difference between the reference signal and measured signal

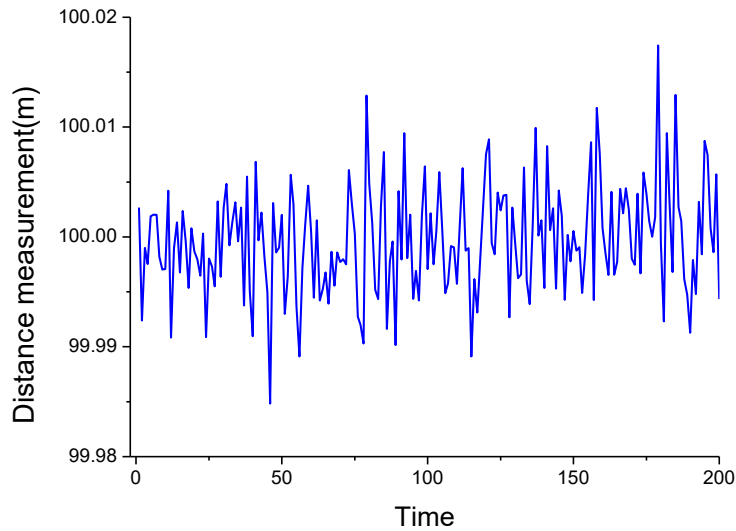


Figure 4-20 Distance measurement result when the ranging distance is 100m

As can be seen in Figure 4-19 and Figure 4-20, the ranging accuracy of single-frequency hybrid pulse and phase-shift laser ranging model depends on phase difference measurement precision. When the ranging distance is 100 m, the maximum ranging error is 1.71cm, the standard deviation of the ranging result is 0.53 cm. Moreover, the ranging distance is simulated for 20.6m, 50m, 500m, 963.15m, and the sampling points are 512, 1024 and 2048 respectively. The standard deviation and the worst case of distance measurement are shown in Table 4-3.

Table 4-3 Simulation results of the single-frequency hybrid pulse and phase-shift laser ranging model

		Distance measurement error(cm)					
		Standard deviation			Worst case		
Distance(m)	Sampling points	512	1024	2048	512	1024	2048
20.6		0.26	0.22	0.15	0.80	0.69	0.55
50		0.35	0.30	0.31	1.65	1.55	1.05
100		0.95	0.66	0.53	2.62	1.82	1.71
500		2.35	2.25	2.19	6.60	5.75	5.85
963.15		3.90	3.78	3.66	16.08	14.6	13.5

As can be seen from Table 4-3, the ranging accuracy of single-frequency hybrid pulse and phase-shift laser ranging model decreases as the ranging distance increases. More sampling points always get better-ranging accuracy. When using the number of sampling points is 2048, the maximum distance error is less than 14 cm, and the ranging standard deviation is less than 3.7 cm. The simulation result can prove the designed dual-frequency hybrid pulse and phase-shift laser ranging system has achieved high ranging accuracy.

4.3 Laser Ranging System Comparison

A performance comparison of the proposed laser ranging works with recently published papers is executed. The performance of simulated laser ranging methods is summarized in Table 4-4 and Table 4-5. The comparison of simulation results with recent two TOF published works are shown in the following tables. Dual-frequency refers to the proposed dual-frequency hybrid pulse and phase-shift laser ranging method and single-frequency corresponds to the proposed single-frequency hybrid pulse and phase-shift laser ranging method.

Table 4-4 The simulation results of the standard deviation of ranging error

		Standard deviation of ranging error(cm)					
		Dual-frequency			Single-frequency		
Distance(m)	Sampling points	512	1024	2048	512	1024	2048
20.6		0.25	0.25	0.23	0.26	0.22	0.15
50		0.36	0.35	0.32	0.35	0.30	0.31
100		0.60	0.56	0.48	0.95	0.66	0.53
500		2.32	2.21	2.15	2.35	2.25	2.19
963.15		3.97	3.72	3.40	3.90	3.78	3.66

Table 4-5 The simulation results of worst ranging error

		Worst ranging error(cm)					
		Dual-frequency			Single-frequency		
Distance(m)	Sampling points	512	1024	2048	512	1024	2048
20.6		0.76	0.65	0.52	0.80	0.69	0.55
50		1.33	1.25	0.93	1.65	1.55	1.05
100		2.05	1.88	1.69	2.62	1.82	1.71
500		6.50	6.35	5.70	6.60	5.75	5.85
963.15		15.7	13.6	12.0	16.08	14.6	13.5

The ranging errors of the dual-frequency case are slightly lower than the single-frequency case. The standard deviation of ranging errors is less than 4 cm, and the worst ranging error is lower than 16.5 cm when using the proposed ranging methods. The result of laser ranging proposed in [35] is shown in Table 4-6. The researchers in [35] use three thresholds to compensate the timing error occurred in the time discriminator.

Table 4-6 Ranging errors reported from [35]

Distance(m)	Standard deviation of ranging error(cm)	Worst ranging error(cm)
20.6	0.4	2.6

The standard deviation of ranging error for 20.6 m is 0.4cm [35] while the proposed dual-frequency method is lower than 0.25 cm and the single-frequency is less than 0.26 cm. Their worst ranging error at 20.6 m can be 2.6 cm [35] compared to the given works with 0.76 cm and 0.80 cm. Both the acquired values for the proposed methods are much better than their works.

For another comparison, the analysts offer a multi-pulse coherent superposition method with 1000 sampling points to improve the measurement precision [93]. Table 4-7 shows the results of the ranging error from this work.

Table 4-7 Ranging errors reported from [93]

Distance(m)	Worst ranging error(cm)
50	3
963.15	15

As can be seen from Table 4-7, the worst ranging error from the paper [93] is lower than those of the proposed works with sampling points of 512. Nevertheless, with the increment of sampling points, the worst ranging error of proposed works are gradually less than this work.

Overall, the proposed dual-frequency and single-frequency hybrid pulse and phase-shift methods have better-ranging precision than currently reported technologies. The ranging results of 20.6 m for proposed methods have higher accuracy than the paper [35] with a standard deviation of 0.4 cm and a worst case of 2.6 cm. In the simulated ranging distance of 963.15 meters, the measurement errors of both methods are less than 16.5 cm, and the standard deviations are less than 4 cm. When the number of sampling points is more than 1024, the ranging results of two proposed method are always better than the published work [93].

What is more, as the number of sampling points increases, the ranging accuracy of the two methods will be further improved which is not possible with conventional pulse ranging method.

4.4 Simulation Summary

The simulation models are established in Optisystem and MATLAB to verify the correctness and feasibility of the designed laser ranging systems. In the simulation experiment, the simulation distance is set to 100 m firstly. The transmitting frequencies of the dual-frequency method are 15 MHz and 150 KHz, and the transmitting frequency of the single-frequency method is 15 MHz. The simulation outcomes are then compared with the recently published works.

According to the simulation results, it can be expected that the designed hybrid pulse and phase-shift laser ranging systems are better than the traditional ranging method. Furthermore, for dual-frequency hybrid pulse and phase-shift laser ranging systems, the theoretical measurement range increases as the laser emission power increases.

Chapter 5 Conclusion

5.1 Thesis Conclusion

Laser ranging technology has widely used in many fields due to its high measurement accuracy and long measuring distance. At present, with the increasing demand for ranging in areas such as civil, scientific research, and military, how to obtain higher measurement accuracy under the premise of ensuring measurement distance has become a favored research area.

At present, both the pulse ranging method and the phase-shift ranging method are the most commonly used laser ranging methods. The pulse method has the advantages of long measurement range and fast measurement speed, and its measurement accuracy is limited. The phase-shift method has the advantage of high measurement accuracy, while the measurement range is restricted by the ambiguous range. Focusing on how to obtain high-precision and long-range laser ranging, in this thesis, the combination of the pulse method and the phase-shift method are discussed, and the theoretical derivation and simulation experiments are completed. The main work of this thesis includes the following aspects:

(1) Firstly, by analyzing the characteristics of the traditional laser ranging methods, several theoretical and fundamental technical problems were studied and discussed in detail. Ranging accuracy of pulse ranging method is limited by the resolution of counting pulse oscillator. There is a contradiction between the ranging distance and the accuracy of the distance measurement for the phase-shift laser ranging system. Since the pulse method and the phase-shift method have similar ranging principles, it has the potential of combining their advantages.

(2) Based on the principle of Fourier series of the pulse signal, two structures of combining the pulse method and the phase-shift method were proposed and analyzed in detail. The system with the dual-frequency measurement signal was introduced. The first structure was the dual-frequency pulse laser ranging method. By transmitting two pulse signals of different frequencies, the results of calculating the phase shift of the same-frequency sinusoidal signals of the two pulse signals at the receiving end were combined to obtain the final measured distance. The second structure was the single-frequency pulse laser ranging method. By transmitting a pulse signal, the

rough distance was acquired by the pulse counting portion, and the phase-shift measurement of co-frequency sinusoidal signals after mixing and filtering was used as the accurate measurement. Then the measurement results were merged to complete the distance measurement.

(3) Because of the unavoidable noise and frequency offset in the actual laser ranging system, the capability of phase difference measurement by using digital synchronous detection, fast Fourier transform method and all phase fast Fourier transform method were simulated in MATLAB. The effects of white Gaussian noise, normalized frequency deviation, harmonics, and sampling points on the accuracy of phase estimation were added in the simulation. The comparison proved that ap-FFT method had higher accuracy than the other two methods.

(4) At the end of the thesis, two proposed models including the laser modulation emission unit, the optical system, the receiving unit and the signal processing unit were established in Optisystem and MATLAB. The tests simulated within one Kilometer. Both two proposed ranging methods achieve a 16.5 cm ranging error with the sampling points of 512. Compared with two recently published works, the proposed methods can realize higher precision in all cases when the number of sampling points was more than 1024. So, improved laser ranging methods have been proposed.

The innovation of this thesis mainly includes the mathematical models of phase difference measurement error based on three commonly used methods. The comparison gave the relationship between the accuracy of the phase difference calculation and normalized spectral deviation, SNR, and harmonic. After that, based on the pulse method and the phase-shift method, two hybrid pulse and phase-shift laser ranging methods were proposed and established in Optisystem and MATLAB. The simulation results agreed with the analysis that designed systems increased the measurement distance and accuracy.

5.2 Future Work

Laser ranging technology is a comprehensive photoelectric detection system and the production and debugging of it are complicated. This thesis is only a preliminary study of the ranging scientific principle and completes the theoretical analysis of the distance measurement system and the algorithm analysis and programming of phase difference measurement. There are

still several aspects need to be optimized for the further research work to achieve high performance and practical value:

In this thesis, the critical technologies of distance measurement of two proposed laser ranging systems are analyzed. The details of them are not involved which is needed to be done in the further research.

Furthermore, the structure of the long-range ranging system has been able to meet the scientific needs while the high-precision and the fast-speed algorithm is worthy for further study and research.

With the development of laser technology and electronic technology, laser ranging will go toward the direction of high precision and broad range. Laser ranging is bound to be more widely used in a variety of fields. Applications of high-precision, long-range laser ranging have many implementation spaces, especially in laser atmospheric communication.

Reference

- [1] R. G. Gould, "The LASER, light amplification by stimulated emission of radiation," *The Ann Arbor conference on optical pumping*, the University of Michigan. Vol. 15. 1959.
- [2] L. A. Coldren, S. W. Corzine and M. L. Mashanovitch, *Diode lasers and photonic integrated circuits*. Vol. 218. John Wiley & Sons, 2012.
- [3] S. Donati, *Electro-optical instrumentation: sensing and measuring with lasers*. Pearson Education, 2004.
- [4] J. L. Gaumet, J. L. Heinrich and M. Cluzeau, "Cloud-base height measurements with a single-pulse erbium-glass laser ceilometer," *Journal of atmospheric and oceanic technology*, 15.1 (1998): 37-45.
- [5] M. Kaoru and H. Matsumoto, "High-accuracy measurement of 240-m distance in an optical tunnel by use of a compact femtosecond laser," *Applied Optics*, 39.30 (2000): 5512-5517.
- [6] Y. K. Cho, C. Wang, P. Tang and C. T. Haas, "Target-focused local workspace modeling for construction automation applications." *Journal of Computing in Civil Engineering* 26.5 (2011): 661-670.
- [7] C. O. Weiss and R. Vilaseca, "Dynamics of lasers," *NASA STI/Recon Technical Report A*, 92 (1991).
- [8] FiberLabs Inc, "What is semiconductor laser diode," [Online]. Available: <https://www.fiberlabs-inc.com/about-semiconductor-laser-diode/>.
- [9] H. -. Rein, R. Schmid, P. Weger, T. Smith, T. Herzog and R. Lachner, "A versatile Si-bipolar driver circuit with high output voltage swing for external and direct laser modulation in 10 Gb/s optical-fiber links," in *IEEE Journal of Solid-State Circuits*, vol. 29, no. 9, pp. 1014-1021, Sept. 1994.

- [10] S. Kumar and M. J. Deen, *Fiber Optic Communications: Fundamentals and Applications*, 1st ed. Chichester, United Kingdom: John Wiley & Sons, Ltd, 2014.
- [11] Z. Wang, Y. Liu, Q. H. Liao, H. Y. Ye, M. Liu and L. J. Wang, "Characterization of a RS-LiDAR for 3D Perception," *arXiv preprint*, arXiv:1709.07641 (2017).
- [12] M. Liu, "Robotic online path planning on point cloud," in *IEEE Transactions on Cybernetics*, vol. 46, no. 5, pp. 1217-1228, May 2016.
- [13] B. Schwarz, "LIDAR: Mapping the world in 3D," *Nature Photonics*, 4.7 (2010): 429-430.
- [14] N. Muhammad and S. Lacroix, "Calibration of a rotating multi-beam lidar," *2010 IEEE/RSJ International Conference on Intelligent Robots and Systems*, Taipei, 2010, pp. 5648-5653.
- [15] J. Levinson and S. Thrun, "Robust vehicle localization in urban environments using probabilistic maps," *2010 IEEE International Conference on Robotics and Automation*, Anchorage, AK, 2010, pp. 4372-4378.
- [16] B. Douillard, A. Brooks and F. Ramos, "A 3D laser and vision based classifier," *2009 International Conference on Intelligent Sensors, Sensor Networks and Information Processing (ISSNIP)*, Melbourne, VIC, 2009, pp. 295-300.
- [17] D. Steinhauser, O. Ruepp and D. Burschka, "Motion segmentation and scene classification from 3D LIDAR data," *2008 IEEE Intelligent Vehicles Symposium*, Eindhoven, 2008, pp. 398-403.
- [18] A. Segal, D. Haehnel and S. Thrun, "Generalized-ICP," *Robotics Science and Systems*, 2009.
- [19] C. L. Glennie, A. Kusari and A. Facchin, "Calibration and Stability Analysis of the VLP-16 Laser Scanner," *ISPRS - International Archives of the Photogrammetry, Remote Sensing and Spatial Information Sciences*, 2016, XL-3/W4:55-60.
- [20] Velodynelidar," HDL-64E." [Onlion]. Available: <https://velodynelidar.com/hdl-64e.html>.
- [21] Wikipedia, "Triangulation." [Onlion]. Available: <http://en.wikipedia.org/wiki/Triangulation>.

- [22] D. J. Harding, M. A. Lefsky, G. G. Parker and J. B. Blair, "Laser altimeter canopy height profiles: Methods and validation for closed-canopy, broadleaf forests," *Remote Sensing of Environment*, 76.3 (2001): 283-297.
- [23] Z. Zhong, J. Tan, H. Chen and H. Ma, "The effect on Doppler frequency shift by measurement prism 3-dimension motion." *Proceedings of SPIE, the International Society for Optical Engineering. Society of Photo-Optical Instrumentation Engineers*, 2005.
- [24] T. B. Eom, T. Y. Choi, K. H. Lee and H. S. Choi, "A simple method for the compensation of the nonlinearity in the heterodyne interferometer," *Measurement Science and Technology*, 13.2 (2002): 222.
- [25] G. Bazin and B. Journet, "A new laser range-finder based on FMCW-like method," *Quality Measurement: The Indispensable Bridge between Theory and Reality (No Measurements? No Science! Joint Conference - 1996: IEEE Instrumentation and Measurement Technology Conference and IMEKO Tec*, Brussels, Belgium, 1996, pp. 90-93 vol.1.
- [26] B. Journet and G. Bazin, "A low-cost laser range finder based on an FMCW-like method," in *IEEE Transactions on Instrumentation and Measurement*, vol. 49, no. 4, pp. 840-843, Aug. 2000.
- [27] D. Dupuy, M. Lescure and M. Cousineau, "A FMCW laser range-finder based on a delay line technique," *IMTC 2001. Proceedings of the 18th IEEE Instrumentation and Measurement Technology Conference. Rediscovering Measurement in the Age of Informatics (Cat. No.01CH 37188)*, Budapest, 2001, pp. 1084-1088 vol.2.
- [28] Green Car Congress, "BMW i Ventures invests in Blackmore Sensors and Analytics, developer of automotive FMCW lidar, " [Online] Available: <http://www.greencarcongress.com/2018/03/20180320-bmwi.html>
- [29] S. B. Gokturk, H. Yalcin and C. Bamji, "A Time-of-Flight depth sensor - system description, issues and solutions," *2004 Conference on Computer Vision and Pattern Recognition Workshop*, Washington, DC, USA, 2004, pp. 35-35.

- [30] A. J. Kilpela, "Pulsed time-of-flight laser range finder techniques for fast, high-precision measurement applications," (2002): 1081-1081.
- [31] T. Ruotsalainen, P. Palojarvi and J. Kostamovaara, "A wide dynamic range receiver channel for a pulsed time-of-flight laser radar," *IEEE Journal of Solid-State Circuits*, 36.8 (2001): 1228-1238.
- [32] J. Nissinen, I. Nissinen and J. Kostamovaara, "Integrated receiver including both receiver channel and TDC for a pulsed time-of-flight laser rangefinder with cm-level accuracy," in *IEEE Journal of Solid-State Circuits*, vol. 44, no. 5, pp. 1486-1497, May 2009.
- [33] S. Kurtti and J. Kostamovaara, "An integrated laser radar receiver channel utilizing a time-domain walk error compensation scheme," in *IEEE Transactions on Instrumentation and Measurement*, vol. 60, no. 1, pp. 146-157, Jan. 2011.
- [34] H. Cho, C. Kim and S. Lee, "A high-sensitivity and low-walk error LADAR receiver for military application," in *IEEE Transactions on Circuits and Systems I: Regular Papers*, vol. 61, no. 10, pp. 3007-3015, Oct. 2014.
- [35] S. Kurtti, J. Nissinen and J. Kostamovaara, "A wide dynamic range CMOS laser radar receiver with a time-domain walk error compensation scheme," in *IEEE Transactions on Circuits and Systems I: Regular Papers*, vol. 64, no. 3, pp. 550-561, March 2017.
- [36] K. Ichiyama, M. Ishida, T. J. Yamaguchi and M. Soma, "A real-time delta-time-to-voltage converter for clock jitter measurement," *2006 IEEE International Test Conference*, Santa Clara, CA, 2006, pp. 1-8.
- [37] S. Fang, Y. Zheng, L. Li, X. Wang, X. Meng and J. Zhao, "A novel time extension method of the pulse laser ranging system," (2015).
- [38] D. Resnati, I. Rech, M. Ghioni, S. Cova, "Monolithic time-to-amplitude converter for photon timing applications," *Proc. SPIE 7355, Photon Counting Applications, Quantum Optics, and Quantum Information Transfer and Processing II*, 73550V (18 May 2009).

- [39] G. H. Li and H. P. Chou, "A high resolution time-to-digital converter using two-level vernier delay line technique," *2007 IEEE Nuclear Science Symposium Conference Record*, Honolulu, HI, 2007, pp. 276-280.
- [40] A. M. Amiri, M. Boukadoum and A. Khouas, "A multihit time-to-digital converter architecture on FPGA," in *IEEE Transactions on Instrumentation and Measurement*, vol. 58, no. 3, pp. 530-540, March 2009.
- [41] T. -. Otsuji, "A picosecond-accuracy, 700-MHz range, Si bipolar time interval counter LSI," in *IEEE Journal of Solid-State Circuits*, vol. 28, no. 9, pp. 941-947, Sept. 1993.
- [42] B. F. Levine, J. A. Valdmanis, P. N. Sacks, M. Jazwiecki and J. H. Meier, "-29dBm sensitivity, InAlAs APD-based receiver for 10Gb/s long-haul (LR-2) applications," *OFC/NFOEC Technical Digest. Optical Fiber Communication Conference, 2005.*, Anaheim, CA, 2005, pp. 3 pp. Vol. 6-.
- [43] M. McClish, R. Farrell, F. Olschner, M. R. Squillante, G. Entine and K. S. Shah, "Characterization of very large silicon avalanche photodiodes," *IEEE Symposium Conference Record Nuclear Science 2004.*, Rome, 2004, pp. 1270-1273 Vol. 2.
- [44] J. Nissinen and J. Kostamovaara, "Wide dynamic range CMOS receivers for a pulsed time-of-flight laser range finder," *Proceedings of the 21st IEEE Instrumentation and Measurement Technology Conference (IEEE Cat. No.04CH37510)*, Como, 2004, pp. 1224-1227 Vol.2.
- [45] T. Ruotsalainen and J. Kostamovaara, "A 50 MHz CMOS differential amplifier channel for a laser range finding device," *Proceedings of IEEE International Symposium on Circuits and Systems - ISCAS '94*, London, 1994, pp. 89-92 vol.5.
- [46] H. Stanley, "The GEOS 3 project," *Journal of Geophysical Research: Solid Earth*, 84.B8 (1979): 3779-3783.
- [47] R. V. Sailor and A. R. LeSchack, "Preliminary determination of the Geosat radar altimeter noise spectrum," *Johns Hopkins APL Technical Digest*, 8.2 (1987): 182-183.

- [48] E. P. W. Attema, G. Duchossois and G. Kohlhammer, "ERS-1/2 SAR land applications: overview and main results," *IGARSS '98. Sensing and Managing the Environment. 1998 IEEE International Geoscience and Remote Sensing. Symposium Proceedings. (Cat. No.98CH36174)*, Seattle, WA, USA, 1998, pp. 1796-1798 vol.4.
- [49] S. Mattei, M. R. Santovito, A. Moccia, "New rangefinder system for microsatellite," *Proc. SPIE 5240, Laser Radar Technology for Remote Sensing, (12 January 2004)*; Coddington, I., et al. "Rapid and precise absolute distance measurements at long range." *Nature photonics*, 3.6 (2009): 351-356.
- [50] S. Liu, J. Tan and B. Hou, "Multicycle synchronous digital phase measurement used to further improve phase-shift laser range finding." *Measurement Science and Technology*, 18.6 (2007): 1756.
- [51] S. M. Nejad, K. Fasihi and S. Olyaei, "Modified phase-shift measurement technique to improve laser-range finder performance," *Journal of Applied Sciences*, 8.2 (2008): 316-321.
- [52] J. G. Webster, "The measurement, instrumentation and sensors handbook on CD-ROM," CRC press, (1999).
- [53] C. Baud, H. T. Béteille, M. Lescure and J. P. Beteilleb, "Analog and digital implementation of an accurate phasemeter for laser range finding," *Sensors and Actuators A: Physical*, 132.1 (2006): 258-264.
- [54] B. Journet, G. Bazin and F. Bras, "Conception of an adaptative laser range finder based on phase shift measurement," *Proceedings of the 1996 IEEE IECON. 22nd International Conference on Industrial Electronics, Control, and Instrumentation*, Taipei, Taiwan, 1996, pp. 784-789 vol.2.
- [55] B. Journet and S. Poujouly, "High-resolution laser rangefinder based on a phase-shift measurement method," *Three-Dimensional Imaging, Optical Metrology, and Inspection IV*, Vol. 3520. International Society for Optics and Photonics, 1998

- [56] H. Liu, A. Ghafoor and P. H. Stockmann, "A new quadrature sampling and processing approach," in *IEEE Transactions on Aerospace and Electronic Systems*, vol. 25, no. 5, pp. 733-748, Sept. 1989.
- [57] S. Poujouly and B. A. Journet, "Laser range-finding by phase-shift measurement: moving toward smart systems," *Machine Vision and Three-Dimensional Imaging Systems for Inspection and Metrology*, Vol. 4189. International Society for Optics and Photonics, 2001.
- [58] H. Yoon and K. Park, "Development of a laser range finder using the phase difference method," *Optomechatronic Sensors and Instrumentation*, Vol. 6049. International Society for Optics and Photonics, 2005.
- [59] S. Kim and C. Nguyen, "On the development of a multifunction millimeter-wave sensor for displacement sensing and low-velocity measurement," in *IEEE Transactions on Microwave Theory and Techniques*, vol. 52, no. 11, pp. 2503-2512, Nov. 2004.
- [60] S. Poujouly and B. Journet, "A twofold modulation frequency laser range finder." *Journal of Optics A: Pure and applied optics*, 4.6 (2002): S356.
- [61] J. F. Munro, "Low-cost laser rangefinder with crystal-controlled accuracy." *Optical Engineering*, 44.2 (2005): 023605.
- [62] S. Poujouly, B. Journet and D. Placko, "Digital laser range finder: phase-shift estimation by undersampling technique," *IECON'99. Conference Proceedings. 25th Annual Conference of the IEEE Industrial Electronics Society (Cat. No.99CH37029)*, San Jose, CA, USA, 1999, pp. 1312-1317 vol.3.
- [63] S. Hwang, J. Jang and K. Park, "Solving 2pi ambiguity problem of a laser scanner based on phase-shift measurement method or long distances measurement," *2012 12th International Conference on Control, Automation and Systems*, JeJu Island, 2012, pp. 1250-1252.
- [64] S. Hwang, J. Jang and K. Park, "Note: Continuous-wave time-of-flight laser scanner using two laser diodes to avoid 2π ambiguity," *Review of Scientific Instruments*, 84.8 (2013): 086110.

- [65] F. X. Jia, J. Y. Yu, Z. L. Ding and F. Yuan, "Research on real-time laser range finding system." *Applied Mechanics and Materials*. Vol. 347. Trans Tech Publications, 2013.
- [66] X. Y. Zheng, C. Zhao, H. Y. Zhang, Z. Zheng and H. Z. Yang, "Coherent dual-frequency lidar system design for distance and speed measurements," *2017 International Conference on Optical Instruments and Technology: Advanced Laser Technology and Applications*, Vol. 10619. International Society for Optics and Photonics, 2018.
- [67] Flight International, "Night moves," [Online]. Available: <https://www.flightglobal.com/pdfarchive/view/1985/1985%20-%203289.html?search=night%20move>.
- [68] M. Mokuno, I. Kawano and T. Suzuki, "In-orbit demonstration of rendezvous laser radar for unmanned autonomous rendezvous docking," in *IEEE Transactions on Aerospace and Electronic Systems*, vol. 40, no. 2, pp. 617-626, April 2004.
- [69] M. C. Amann, T. M. Bosch, M. Lescure, R. A. Myllylae and M. Rioux, "Laser ranging: a critical review of usual techniques for distance measurement." *Optical engineering*, 40.1 (2001): 10-19.
- [70] M. Ohishi, F. Ohtomo, M. Yabe, M. Kanokogi, T. Saito, Y. Suzuki and C. Nagasawa, "High-resolution rangefinder with a pulsed laser developed by an undersampling method." *Optical Engineering*, 49.6 (2010): 064302.
- [71] X. J. Wu, A. I. Zhang, Z. R. Tong and Y. Cao, "High precision laser ranging by combining phase method and multi-cycle pulse method," *10th International Conference on Optical Communications and Networks (ICOON 2011)*, Guangzhou, 2011, pp. 1-2.
- [72] Wikipedia, "Square_wave," [Online]. Available: https://en.wikipedia.org/wiki/Square_wave
- [73] J. Shan and C. K. Toth, "Topographic laser ranging and scanning: principles and processing," *CRC press*, 2018.

- [74] C. Brenner, "Digital Recording and 3D Modeling," *Aerial laser scanning. International Summer School*, (2006).
- [75] A. Wehr and U. Lohr, "Airborne laser scanning—an introduction and overview," *ISPRS Journal of photogrammetry and remote sensing*, 54.2-3 (1999): 68-82.
- [76] P. Horowitz and W. Hill, *The Art of Electronics 2nd Ed.* Cambridge University Press, Cambridge, 1989 ISBN 0-521-37095-7 pg. 644
- [77] O. Y. Mang, C. Y. Huang and J. W. Chen, "High-dynamic-range laser range finders based on a novel multimodulated frequency method," *Optical Engineering*, 45.12 (2006): 123603.
- [78] Y. Liu, W. Su, L. Wang and M. Wang, "Phase-laser ranging system based on digital signal processing for optoelectronics theodolite application," *2010 3rd International Conference on Advanced Computer Theory and Engineering (ICACTE)*, Chengdu, 2010, pp. V2-248-V2-252.
- [79] H. X. Hong and Z. Lin, "An improved algorithm and its application to sinusoid wave frequency estimation," *International Journal of Advanced Computer Science*, 02(06): pp. 217-221, june 2012.
- [80] W. Kester, Walt, ed. *Practical Analog Design Techniques*, Analog Devices, 1995.
- [81] S. Bochner and K. Chandrasekharan. *Fourier Transforms.* (AM-19), Vol. 19. Princeton University Press, 2016.
- [82] A. K. Singh and K. S. Rao. "An algorithm for the interception and analysis of pulse compression radar signals by digital receiver," *International Journal of Darshan Institute on Engineering Research and Emerging Technology*, 02(02): pp. 18-22, 2013.
- [83] E. Aboutanios and B. Mulgrew, "Iterative frequency estimation by interpolation on Fourier coefficients," in *IEEE Transactions on Signal Processing*, vol. 53, no. 4, pp. 1237-1242, April 2005.

- [84] K. Ding, C. S. Zheng and Z. J. Yang, "Frequency estimation accuracy analysis and improvement of energy barycenter correction method for discrete spectrum," *Journal of Mechanical Engineering*, 46.5 (2010): 43-48.
- [85] J. Schoukens, R. Pintelon and H. Van Hamme, "The interpolated fast Fourier transform: a comparative study," in *IEEE Transactions on Instrumentation and Measurement*, vol. 41, no. 2, pp. 226-232, April 1992.
- [86] S. C. Zhong and K. Ding, "A universal phase difference correcting method on discrete spectrum," *Acta Electronica Sinica*, 2003, 31(1):142-145
- [87] A. Boughambouz, A. Bellabas, B. Magaz, T. Menni and M. E. M. Abdelaziz, "Improvement of radar signal phase extraction using All Phase FFT spectrum analysis," *2017 Seminar on Detection Systems Architectures and Technologies (DAT)*, Algiers, 2017, pp. 1-4.
- [88] X. H. Huang, Z. H. Wang and G. Q. Chou, "New method of estimation of phase, amplitude, and frequency based on all phase FFT spectrum analysis," *2007 International Symposium on Intelligent Signal Processing and Communication Systems*, Xiamen, 2007, pp. 284-287.
- [89] A. H. Elghandour and D. R. Chen, "Modeling and comparative study of various detection techniques for FMCW LIDAR using Optisystem," *International Symposium on Photoelectronic Detection and Imaging 2013: Laser Sensing and Imaging and Applications*, Vol. 8905. International Society for Optics and Photonics, 2013.
- [90] D. V. Lee, "Metal compensated radio frequency identification reader". U.S. Patent No. 6,377,176. 23 Apr. 2002.
- [91] M. O. Yang, C. Y. Huang and J. W. Chen, "Method and apparatus of multi-modulation frequency laser range finder," *USA and Taiwan patent pending Jan*, 2005.
- [92] T. Bosch and M. Lescure, "Crosstalk analysis of 1 m to 10 m laser phase-shift range finder," in *IEEE Transactions on Instrumentation and Measurement*, vol. 46, no. 6, pp. 1224-1228, Dec. 1997.

- [93] H. Shi, L. Yu, C. Wang, Y. Yu, X. Liu and L. Li, "Study on multi-pulse long range laser ranging system," *2017 29th Chinese Control And Decision Conference (CCDC)*, Chongqing, 2017, pp. 4838-4843.